Improving socio-ecological management of hydropower systems under climate change

A Thesis Presented to
The Faculty of of the School of Engineering and Applied Science
University of Virginia

In Partial Fulfillment
of the Requirements for the Degree
of Master of Science

Department of Engineering Systems and Environment

By
Sarah Jordan
August 2021

ACKNOWLEDGMENTS

First and foremost, I would like to thank Dr. Julianne Quinn for mentoring me over the past two years. I sincerely appreciate your guidance and encouragement throughout this process. Thank you to my committee members, Dr. Venkataraman Lakshmi, Dr. Jonathan Goodall, and Dr. Teresa Culver for your support in these final stages and for the excellent classes I got to take with each of you. I would also like to thank Dr. Marta Zaniolo, Dr. Matteo Giuliani, and Dr. Andrea Castelletti for introducing me to the Omo River basin, giving me as much data for the area as possible, and providing constructive feedback on my work.

This experience would not have been the same without the other members of the Quinn Group: Samarth Singh, Hossein KavianiHamedani, Jared Smith, and Daniel Lassiter. Thank you for the support, friendship, and fun times in and out of the office. I am excited to see what you do with your research in the next few years.

To my friends and family, thank you for supporting me through the ups and downs of graduate school.

I would also like to acknowledge and thank Jared Oyler for his public debiasing and downscaling code, which made much of this work possible (https://github.com/scrim-network/red_river), and Liang-Jun Zhu, whose Github allowed us to update SWAT source code and create a Linux-compatible executable so we could run this model on Rivanna (https://github.com/WatershedModels/SWAT).

ABSTRACT

Dams and storage reservoirs provide a source of water supply, irrigation, renewable energy, and flood protection in river basins around the world. However, human regulation of river systems alters natural hydrologic patterns, which can adversely impact downstream water users and ecological resources. Developing resilient, robust, and adaptive reservoir controls that can balance social, economic, and ecologic outcomes is an essential, yet challenging task. Impact assessments of alternative reservoir operations under a range of possible future scenarios will be essential to inform the design of robust, integrated reservoir control rules.

This study advances the representation of reservoir operations in the Soil & Water Assessment Tool (SWAT) by integrating nonlinear, multi-reservoir control rules into the model. We consider the Omo River basin of Ethiopia as a case study for the advanced reservoir module, where controversial dam construction provides opportunities for hydropower and irrigation at the expense of indigenous people and aquatic wildlife. We use Evolutionary Multiobjective Direct Policy Search (EMODPS) to optimize reservoir controls that balance the conflicting needs of these stakeholders using both existing SWAT operating rules and our advanced nonlinear control rules. We then perform an impact assessment using the updated reservoir module under alternative climate scenarios to identify policies that continue to balance socio-ecological tradeoffs while mitigating high and low flow extremes under climate change. We find that our advanced operations can better balance conflicting multisectoral needs than existing reservoir operations in SWAT under both historical and climate change conditions, and that our updated policies can mitigate the impact of climate change on high and low flow extremes while continuing to balance socio-ecological tradeoffs.

CONTENTS

LIST OF TABLES

LIST OF FIGURES

LIST OF SYMBOLS AND ABBREVIATIONS

7Q10	Seven-day, ten-year low flow
7QS	Annual seven-day minimum flow series
ABM	Agent Based Model
AMS	Annual Maxima Series
ANN	Artificial Neural Network
CASAA ...	Constructed Analogs with Single Anomaly Analog
CCI	Climate Change Initiative
CHIRPS ...	Climate Hazards group InfraRed Precipitation with Station
CMIP5	Coupled Model Intercomparison Project 5
DDS	Dynamically Dimensioned Search
DEM	Digital Elevation Model
DPS	Direct Policy Search
ECDF	Empirical Cumulative Distribution Function
EDCDFm ..	Equidistant Cumulative Distribution Function Matching
EEPCO ...	Ethiopian Electric Power Corporation
EMODPS ..	Evolutionary Multi-Objective Direct Policy Search
ESA	European Space Agency
ESC	Ethiopian Sugar Corporation
ESIA	Environmental and Social Impact Assessment
FAO-UNESCO	Food and Agriculture Organization of the United Nations
GCM	General Circulation Model
GWh	Gigawatt-hour

HPC	High Performance Computing
HUC	Historical uncontrolled
ITCZ	Inter-Tropical Convergence Zone
MEF	Minimum Environmetal Flow
MOEA ...	Multi-Objecitve Evolutionary Algorithm
NFE	Number of Function Evaluations
NL	Nonlinear
NSE	Nash-Sutcliffe Efficiency
PUC	Projected uncontrolled
RBF	Radial Basis Function
RC	Rule Curve
RCP	Representative Concentration Pathways
SPAM	Spatial Production Allocation Model
SRTM	Shuttle Radar Topography Mission
SWAT	Soil & Water Assessment Tool
TOPKAPI ..	TOPographic Kinematic APproximation and Integration

CHAPTER 1

Introduction

Economic development, population growth, and climate change have triggered an increase in global dam construction as a source of domestic water supply, irrigation, and renewable energy (Zarfl et al., 2015; Suen & Eheart, 2006). The economic benefits associated with dams have historically been the primary drivers in decisions about how and when water is released from reservoirs (Hurford & Harou, 2014; Ho et al., 2017). However, this approach often benefits private companies and governments while placing the costs of hydropower development on local communities and the environment, resulting in steep social and ecological consequences (Zarfl et al., 2015). Maximizing the economic benefits of water releases from reservoirs disrupts natural flow regimes, which can fragment free-flowing rivers (Graf, 2001), severely alter or destroy aquatic ecosystems (Liermann et al., 2012; Poff & Hart, 2002; Goodland, 2010), restrict access to water resources, cause transboundary conflicts (Zarfl et al., 2015), and modify water quality (Gyasi et al., 2018). Furthermore, dam construction has displaced 40-80 million people worldwide, disproportionately affecting indigenous populations (Goodland, 2010; Babbitt, 2002). Climate change is only projected to exacerbate these multisectoral conflicts in the future (Poff et al., 2016).

Recent work has focused on integrating economic, social, and environmental objectives into dam management and planning in order to define adaptive reservoir operations that can balance multisectoral water demands and improve both economic and socio-ecological outcomes as the climate changes (Zarfl et al., 2015; Watts et al., 2011; Olden et al., 2014; Wild et al., 2019). Multi-objective optimization has been used to define reservoir operating policies that identify trade-offs between conflicting water users and guide decision makers towards options that are economically viable while still balancing

a range of social and environmental needs (Yu et al., 2021; Li et al., 2017; Quinn et al., 2018). Evolutionary Multi-Objective Direct Policy Search (EMODPS) is a simulation-based optimization approach that can be used to define reservoir operating policies with nonlinear approximators, creating state-dependent reservoir operating rules that can effectively adapt to changing system conditions (Giuliani et al., 2016b). However, many reservoir simulation models used for EMODPS are relatively simplistic representations of river systems that lack the information needed to adequately represent socio-ecological outcomes and coupled natural-human system dynamics.

The Soil & Water Assessment Tool (SWAT) is a semi-distributed, physically-based hydrologic model that can simulate a wide range of natural processes, including hydrology, nutrient cycling, plant behavior, and climate change, as well as the impact of anthropogenic activities on these natural systems (Arnold et al., 2012). It is therefore a powerful tool for quantifying economic, agricultural, hydrologic, and environmental outcomes to assess the performance of alternative integrated water resources management strategies. Furthermore, numerous studies have paired SWAT with agent based models (ABMs) to simulate coupled natural-human system feedbacks (Khan, 2018). However, SWAT2012's reservoir module is limited and overly simplistic, particularly for river basins where reservoir operations have a significant influence on downstream hydrology.

In this thesis, we advance the representation of reservoir operations in SWAT so that we can simulate more adaptive reservoir operating policies that can better balance socio-ecological tradeoffs than existing reservoir operations in the model. This will enable users interested in integrated reservoir management to fully leverage the model's ability to capture coupled natural-human systems dynamics. We then use the updated reservoir module to simulate these adaptive policies under a range of climate scenarios to assess whether reservoir operations can mitigate flow extremes while balancing economic, so-

cial, and ecological outcomes, or if they exacerbate conflicts. We find that policies favoring extreme outcomes on one objective often do so at the expense of others, but that our approach is also able to identify compromise solutions that mitigate ecological high and low flow extremes while providing additional socio-economic benefits. Our advancements show promise for informing adaptive integrated water resources management strategies capable of balancing conflicting, multi-sectoral needs under climate change.

CHAPTER 2

Advancing reservoir operations in the Soil and Water Assessment Tool to reduce socio-ecological tradeoffs

2.1 ABSTRACT

The Soil & Water Assessment Tool (SWAT) is a useful model for evaluating socio-ecological tradeoffs and analyzing coupled natural-human system dynamics in large agricultural watersheds. However, reservoir operating rules in SWAT are limited to three simple modules. This study advances the representation of reservoir operations in SWAT by integrating alternative nonlinear and closed-loop, multi-reservoir operating policies into the model and optimizing them using Evolutionary Multi-Objective Direct Policy Search (EMODPS). This enables water managers to evaluate the tradeoffs of more complex reservoir operations in SWAT while capitalizing on SWAT's ability to model both natural and human outcomes in river systems better than traditional reservoir simulation models. As a case study for this integration, we consider the Omo River basin of Ethiopia, where controversial dam construction is creating opportunities for hydropower and irrigation, but proving detrimental to indigenous people and aquatic wildlife dependent on natural flows and sufficient water levels in Lake Turkana downstream. Comparing our advanced reservoir operations with SWAT's existing operating options, we find a wider range of policies for managing these conflicting stakeholder objectives that better compromise across them. This also aids in the identification of policies that are more robust to climate change. Our advances in the reservoir module of SWAT show promise for informing integrated water resources management in the Omo and other river basins.

2.2 INTRODUCTION

Socio-ecological systems models are powerful tools for simulating interactions between human and natural systems to understand their vulnerabilities to different natural resources management policies and climatic stressors. Within the water resources literature, the Soil & Water Assessment Tool (SWAT) has emerged as the dominant tool for simulating these interactions in agricultural systems. SWAT is a semi-distributed, physically-based watershed model capable of modeling surface and subsurface hydrology, sediment transport, plant growth, and nutrient dynamics (Figure 2.1). The model was designed to enable users to evaluate the effects of alternative management decisions on water resources in large river basins (Arnold et al., 2012). Users can simulate crop planting, harvesting, irrigation and pesticide applications, tillage operations, and reservoir management to observe the impact that these human actions have on the natural system. These include water quality impacts of erosion, sedimentation, and polluted runoff such as loads of nutrients, pesticides, bacteria, and biochemical oxygen demand (BOD), as well as water quantity impacts of changing hydrologic variability and seasonality.

Not only can SWAT model one-way impacts of human decisions on the environment, but its open source code allows for integration of SWAT with agent based models (ABMs) and other decision support tools that enable two-way feedbacks between human decisions and environmental outcomes (Khan, 2018). This allows modelers to simulate how humans may change their future management decisions in response to past decisions' environmental impacts, investigating how those two-way interactions propagate to socio-environmental outcomes.

A major water management strategy humans might change in response to observed environmental outcomes, and in particular under climate change, is reservoir operations. However, the representation of reservoir operations in SWAT2012 is simplistic and lim-

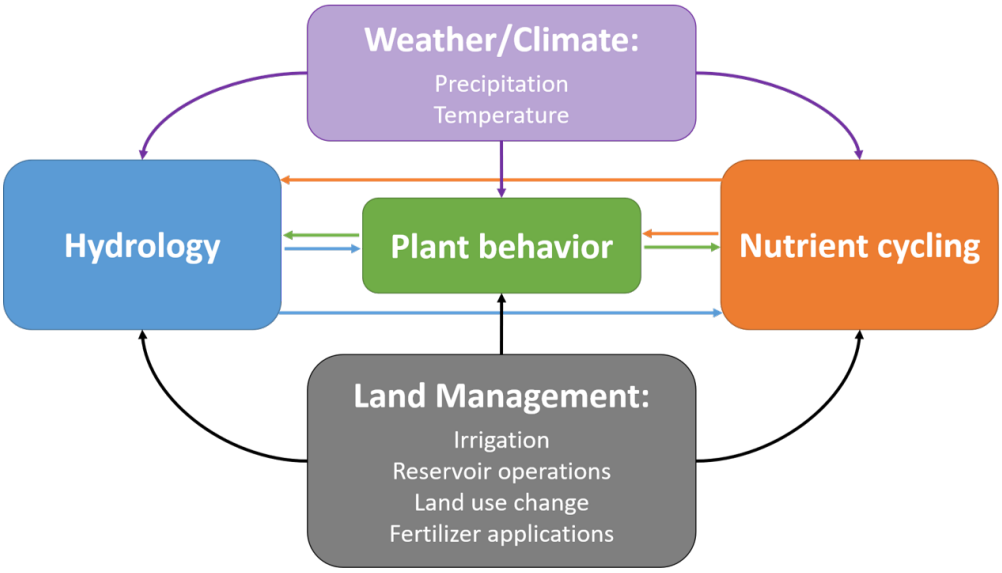

Figure 2.1: SWAT can model the interactions between components of the natural system (hydrology, plant behavior, nutrient cycling, and climate) and human decisions. Adapted from Lee et al. (2017) and (Neitsch et al., 2011)

ited (Wu et al., 2020). In the existing reservoir module, users can input measured daily or monthly releases if historical information is available, but this doesn't allow users to model how reservoirs might operate in the future. For small, uncontrolled reservoirs, users can simply define an average daily water release rate. However, many agricultural systems around the world are fed by large surface reservoirs with more variable operations. These include mega-dams in the American West, as well as recent hydropower development focused in Asia, Latin America, and Africa aimed at increasing electrification through hydropower production while also providing access to irrigation in areas with developing economies (Zhang et al., 2018). To model large reservoirs like these, users can define monthly reservoir target storages in SWAT (Neitsch et al., 2011).

While many reservoirs operate according to simple rules like these, federal agencies are recognizing the value of more complex, adaptive rules and are becoming more open to integrating them into operations (Jasperse et al., 2017; Talbot et al., 2017). Recent advance-

ments in multi-objective optimal control methods have enabled the discovery of more complex reservoir operating rules that can better balance conflicting socio-ecological outcomes, adapt to system variability, or mitigate the impact of climate change, all of which are essential for integrated reservoir management (Giuliani et al., 2016b; Zaniolo et al., 2021). However, applications of these advanced methods have been limited to reservoir systems models that do not physically model the rainfall-runoff process or the ecological impacts of alternative operations. This requires coupling multiple models to understand how changing climate conditions propagate through to water supply impacts (see e.g. Giuliani et al. (2016a); Zaniolo et al. (2021); Steinschneider & Brown (2012)), or how water supply impacts propagate to agro-ecological impacts (see e.g. Georgiou & Papamichail (2008)). Alternatively, the reservoir simulation models rely on non-physical representations of processes like erosion and sedimentation (Schmitt et al., 2018), or proxy measures of agro-ecological impacts like water supply deficits (Loucks & van Beek, 2017).

This study seeks to overcome the shortcomings of SWAT in modeling reservoir operations, and of reservoir simulation models in physically modeling interactions between human and natural systems by advancing the representation of reservoir operations in SWAT. We update the SWAT source code to enable the simulation and optimization of closed-loop, nonlinear, and state-aware reservoir operating policies designed with Evolutionary Multiobjective Direct Policy Search (Giuliani et al., 2016b). We apply these updated policies to a multiobjective, multireservoir control problem in the Omo River basin, where a series of reservoirs must balance the irrigation needs of largescale agriculture with the downstream flow requirements of indigenous people and aquatic wildlife, while still generating enough electricity output to justify the cost of hydropower development. We compare the performance of existing reservoir operations in SWAT with the updated operations under historical and possible future climate conditions to see if we can define

more resilient and robust management strategies that reduce socio-ecological tradeoffs under a range of conditions. We find more of the nonlinear operating rules are able to outperform uncontrolled operations than the simple SWAT operations across all system objectives in all climate projections due to their ability to adapt operations in response to changing climate inputs. Future work can explore how these alternative operating policies interact with alternative agricultural management strategies that may increase or decrease erosion and sedimentation or change optimal irrigation needs, requiring additional adaptation of reservoir operations.

2.3 CASE STUDY

2.3.1 Omo Background

The Omo River basin is a 79,000 km^2 watershed in southwestern Ethiopia that drains from the humid Shewan highlands to the hot and arid Lower Omo Valley where it forms a biodiverse delta at the Ethiopia-Kenya border. The river terminates at Lake Turkana in Kenya, which is the world's largest desert lake, spanning over 130,000 km^2 (Figure 2.2); Avery, 2012). Historically, the Omo River basin has been a pastoral region where nomadic indigenous tribes migrate seasonally based on water and food availability, which are controlled by the river's monsoonal flows. As the Inter-Tropical Convergence Zone (ITCZ) shifts northward from September to November and southward from March to May, it brings with it rains that result in alternating wet and dry seasons (SOGREAH, 2010). Rainfall in the northern Omo Basin peaks in August with a long, dry season from November to March; rainfall in the central Omo Basin exhibits a longer and less intense wet season from April to September; and rainfall in the southern Omo features two mildly rainy periods, one in March and April and another in September and October. Total annual precipitation is highly variable throughout the watershed, ranging from about 1,900

mm/year in the northernmost parts of the basin to just 300 mm/year in the southern Omo near Lake Turkana.

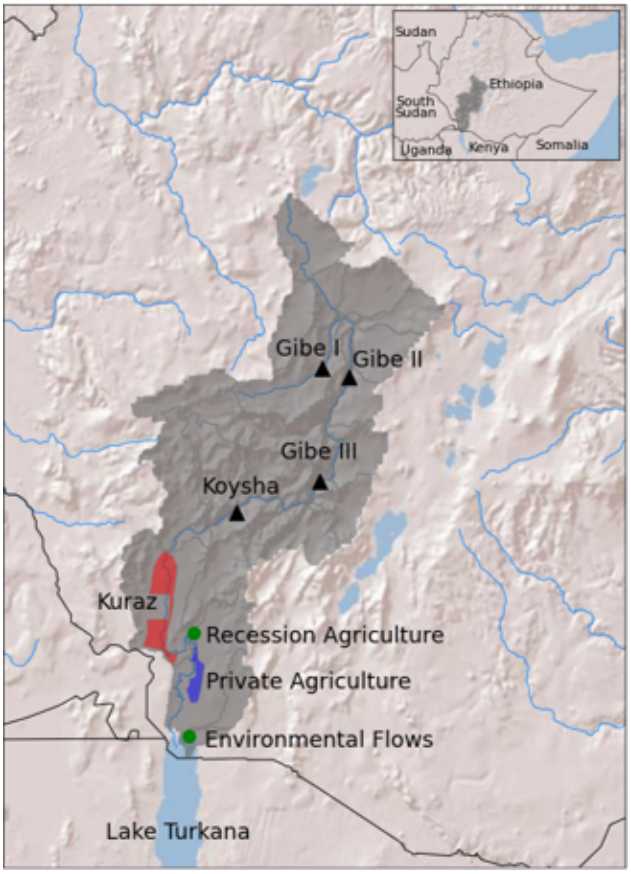

Figure 2.2: Map of the Omo River Basin, including all hydropower dams, planned irrigated agricultural developments, and approximate locations where flood recession agriculture is practiced and environmental flows should be met.

However, the historical flow pattern induced by these monsoonal rains is being altered by dam construction for hydropower production and the expansion of irrigable agriculture in the basin (Woodroofe, 1996). The Omo River Basin has been a major target for hydropower projects because of its high hydropower potential: large amounts of concentrated rainfall in the basin's highlands creates the second largest annual runoff of any river system in the country (Avery, 2012). Furthermore, the Omo River is steep, flowing

from an elevation of about 3,000 m in the highlands to 400 m at Lake Turkana over its 760 km length.

Three power plants have been constructed in the Omo River basin over the past 20 years (Gilgel Gibe I, II, and III), with another hydropower plant (Koysha) under construction (Table 2.1). This water infrastructure development has been extremely controversial in the Omo River basin since it promotes economic development at the expense of indigenous people and ecological resources. The Gibe III dam has been particularly controversial as questions surround the legitimacy of its Environmental and Social Impact Assessment (ESIA), and downstream flows significantly reduced during its filling phase and first few years in operation, resulting in steep social impacts (Carr, 2017a; Avery, 2012, 2014).

Table 2.1: Hydropower development in the Omo River basin.

Name	Years of Construction	Capacity (MW)	Height (m)
Gibe I	1999-2004	184	40
Gibe II (power plant)	2004-2009	420	550
Gibe III	2006-2015	1870	250
Koysha	2016-present	2160	178.5

Continued hydropower development is planned in the Omo River basin with the Koysha dam. Ethiopia is working towards reaching self-sufficiency in electricity production and 100% electricity access by 2025, with an end goal of becoming an energy exporter (IEA, 2016; Asress et al., 2013; Woodroofe, 1996). As of 2016, the national electrification rate in Ethiopia was just 25%, leaving 75% of the population, mainly those in rural areas like the Omo River basin, without access to electricity (IEA, 2016). Expanding hydropower plants in the Omo helps the country work towards its ambitious goals, and the large storage reservoirs behind the dams enable more reliable electricity output in this

arid region where 90% of the annual runoff is concentrated to just four months of the year (Sundin, 2017).

The storage reservoirs have also allowed for cultivation of large areas devoted to irrigable agriculture (Avery, 2012). The state-owned Ethiopian Sugar Corporation (ESC) is developing the Kuraz Sugar Plantation downstream of the Koysha dam, which is currently projected to span 175,000 hectares. The ESC aims to transform Ethiopia from a sugar importer to a top ten global exporter (Davidson, 2015). The Ethiopian Ministry of Agriculture and Natural Resources has also leased approximately 85,000 hectares of land south of the Kuraz Sugar Development Project to foreign and private investors (Oakland Institute, 2011). This land will primarily be used for cotton plantations (Carr, 2017a; Hodbod et al., 2019). These projects divert water from the main channel through irrigation canals, enabling crop growth in an area that is too dry to support rain-fed agriculture (Human Rights Watch, 2017).

While water infrastructure development has promoted economic growth through hydropower production and the expansion of irrigable agriculture, it has negatively affected indigenous people and the ecological resources in the Lower Omo Valley (Hathaway, 2009; Abbink, 2012; Fratkin, 2014). The lower Omo Basin has historically been home to over 500,000 indigenous people, and the development of large-scale agriculture has resulted in the displacement and abuse of many indigenous communities (Oakland Institute, 2019). The indigenous groups that remain downstream of these developments rely on the Omo River as their primary source of water and food, but altered hydrology from the dams and irrigation diversions have adversely impacted these resources (Carr, 2017a). Approximately 200,000 indigenous people in the Lower Omo Valley practice flood-recession agriculture as a primary source of food. This practice uses the annual flood pulse from the Omo River as a form of irrigation, since the dry conditions in the

Lower Omo cannot support rain-fed agriculture (Carr, 2017a). At the start of the wet season in July, the Omo River starts to rise in the Omo Valley until it floods in August and September, depositing silt on the floodplain. Once the flood recedes, the shores of the River can be cultivated to produce maize and sorghum that serve as the primary food source for the tribes (Carr, 2017a; SOGREAH, 2010; Johnston, 2009). Water infrastructure development has dampened this flood pulse, increasing the likelihood that there will be inadequate area to cultivate crops in any given year, resulting in food shortages among indigenous populations.

The dams have also altered the natural annual hydrologic cycle in the Omo River delta, which feeds into Lake Turkana, an endorheic lake that serves as a food and water source for another 300,000 indigenous people in Ethiopia and Kenya. The Omo River accounts for 90% of total inflows, so flow patterns in the Omo River and water levels in Lake Turkana are directly correlated (SOGREAH, 2010). The historical flood pulse supports the biodiversity in the delta and ensures fluctuations in Lake Turkana's levels, which enable nutrient circulation, support the spawning cycles of fish, and replenish grazing land for livestock along the shores of the lake (Gownaris et al., 2015; Carr, 2017a; Avery, 2012, 2014). Continued disruption to Lake Turkana's natural oscillations could result in widespread food and water shortages and exacerbate conflicts between tribes over limited resources (Carr, 2017a).

In this study, we seek to find reservoir operating policies that balance all these conflicting demands on the Omo River basin's water resources using the Soil & Water Assessment Tool.

2.3.2 SWAT Model

The Soil & Water Assessment Tool is a semi-distributed, physically-based river basin model (Arnold et al., 1998). SWAT is one of the most widely used watershed-scale models because it can simulate a range of hydrologic and environmental processes; it can model hydrological processes, sediment transport and routing, nutrient and pesticide transport, plant growth, climate change, and anthroprogenic features and activities (Gassman et al., 2014). Because it can model the interactions between natural and human processes, it is an excellent tool for assessing the impact of alternative water management strategies on a variety of stakeholders.

We build a SWAT model of the Omo River Basin that includes all constructed and planned hydropower plants and planned irrigable agricultural developments in the region. Unfortunately, precipitation and streamflow data in the basin are limited and not open access. We seek to create as accurate a model as possible given these data limitations, but caution that the model should be further validated and refined as more data become available before any concrete recommendations are made to decision-makers in the Omo River basin. The current formulation still represents a realistic case study for demonstrating the capabilities of updated SWAT reservoir operations in managing socio-ecological tradeoffs.

Data. The 30-meter digital elevation model (DEM) from the NASA Shuttle Radar Topography Mission (SRTM) is used for watershed delineation in SWAT (NASA JPL, 2013). The locations of the four dams on the Omo River (Gibe I, Gibe II, Gibe III, and Koysha) are placed during the delineation phase in SWAT. This divides the Omo River Basin into 27 subbasins.

Land cover data from the European Space Agency (ESA) Climate Change Initiative (CCI) (ESA, 2017) is enhanced using the crop map from the Spatial Production Allocation

Model (SPAM) (HarvestChoice, 2014). The original land cover map is used for calibration purposes, but is then altered to include sugarcane at the Kuraz Sugar Development Project and cotton at privately leased agricultural land using approximate boundaries of these areas defined by the Human Rights Watch (2017), derived from Landsat satellite imagery. Soil data is from the Food and Agriculture Organization of the United Nations' (FAO-UNESCO) Harmonized World Soil Dataset (Nachtergaele et al., 2009).

Meteorological data from weather stations is difficult to access in Ethiopia, and weather stations in the Omo River Basin are sparse. Consequently, we obtain precipitation and temperature data from remotely sensed datasets. Daily precipitation information comes from the Climate Hazards Group InfraRed Precipitation with Station (CHIRPS) dataset at 0.05 degree resolution (Funk et al., 2015). CHIRPS is a quasi-global dataset that spans from 50 degrees south to 50 degrees north. CHIRPS merges satellite observations with data from in-situ precipitation gauges (Funk et al., 2015). Daily precipitation inputs for the SWAT model are calculated by taking a spatial average over each subbasin in the model. Since we are unable to obtain gauge data, we cannot bias-correct CHIRPS data in the Omo River basin, but comparison to historical averages in the literature suggests that the spatial variability, seasonal trends, and overall magnitude of monthly precipitation are reasonable (SOGREAH, 2010).

Air temperature data comes from Copernicus's ERA5-Land reanalysis dataset at a 0.1-degree spatial resolution and hourly temporal resolution (Copernicus Climate Change Service, 2019). The hourly data is resampled to create a 0.1-degree minimum daily temperature and 0.1-degree maximum daily temperature dataset. We use area-to-area cokriging to produce subbasin-level estimates of daily minimum and maximum temperature from the 0.1-degree datasets for SWAT weather input (Hu & Huang, 2020).

Calibration. Streamflow data is sparse and difficult to obtain in the Omo River Basin

(Avery, 2012). Because we lack gauged streamflow data, we calibrate the SWAT model to simulated streamflow values from a TOPographic Kinematic APproximation and Integration model of the basin from researchers at ETH Zurich (TOPKAPI-ETH; Ragettli et al., 2014). TOPKAPI-ETH is a fully spatially distributed and physically based rainfall-runoff model that has been modified for applications to mountainous basins. The Omo TOPKAPI-ETH model is calibrated to lake levels in Lake Turkana (Zaniolo et al., 2021). The calibration period ranges from 2001, the first year with data from the TOPKAPI-ETH model, to 2004, before any dams were operational on the river. Once obtained, data prior to 2001 can be used for validation. For the calibration trials, the reservoirs are set to be inactive and land use is set to its original state (i.e. does not include sugar and cotton development and associated irrigation practices).

We perform 20 calibration trials in parallel over a 24-hour period using the Dynamically Dimensioned Search (DDS) algorithm, an efficient and robust method for automatically calibrating highly parameterized hydrologic models like SWAT (Tolson & Shoemaker, 2006). The calibration objective function seeks to minimize the sum of log-space squared errors in daily flows across the four dam locations and the basin outlet at Lake Turkana (Eqn. 2.1). This favors better fits at downstream points with higher flows where our objectives are most relevant, but more equally weights high and low flows at each location to best fit the full distribution.

$$min \sum_{k=1}^{K} \sum_{t=0}^{T-1} \left(\ln \left(q_{t,k}^{TOPKAPI} \right) - \ln \left(q_{t,k}^{SWAT} \right) \right)^2 \tag{2.1}$$

Here K is the number of locations we are calibrating to (5: Gibe I, Gibe II, Gibe III, Koysha, and Lake Turkana); T is the simulation horizon (1,096 days); $q_{t,k}^{SWAT}$ is the flow simulated by SWAT on day t at location k, and $q_{t,k}^{TOPKAPI}$ is the same for TOPKAPI-ETH.

We select parameters from the calibration trial with the lowest objective value. Visual

inspection of the search progress suggested it had converged (see Figure A.1). All calibration parameters and their final calibrated values are in Table A.1. Model performance is assessed using four statistical indicators: Nash-Sutcliffe Efficiency (NSE), and all of its components, as decomposed in Gupta et al. (2009): relative variance (α), relative bias (β_n), and correlation coefficient (r). Values closer to 1 are preferred for NSE, α and r, while values closer to 0 are preferred for β. All metrics indicate that the model is good to very good for monthly model output (Table 2.2); (Arnold et al., 2012). Poorer fits on the daily time step could be due to the use of different rainfall products between the two models, but are less consequential for our objectives (see 2.4.3).

Table 2.2: Calibration statistics at a daily and monthly timestep.

	Daily				**Monthly**			
Location	*NSE*	α	β_n	r	*NSE*	α	β_n	r
Gibe I	0.53	1.04	0.10	0.78	0.78	1.18	0.125	0.93
Gibe II	0.50	1.32	0.21	0.90	0.74	1.34	0.22	0.96
Gibe III	0.71	1.06	0.12	0.87	0.90	1.05	0.16	0.97
Koysha	0.33	1.20	0.30	0.77	0.76	1.13	0.31	0.95

These calibration statistics indicate that our SWAT model has a wet bias compared to the TOPKAPI-ETH model ($\beta_n > 0$). However, we observe a dry bias relative to the Ethiopian Electric Power Corporation's (EEPCO) reported flows in their ESIA (EEPCO, 2009). We believe that flows that fall inbetween these two observations is reasonable. EEPCO's ESIA has been criticized for its omission, misrepresentation, or erroneous use of environmental data (Carr, 2017b). Since dam construction had already commenced at the time of the report, EEPCO had an incentive to report high flows for accelerated project approval. Furthermore, our peak flows are more in line with those reported in literature in the Lower Omo than the TOPKAPI-ETH model (Avery, 2010).

We also simulate sugarcane yields in the Kuraz Sugar Plantation and cotton yields in the private agricultural area downstream. We cannot calibrate these yields because they are planned developments, but we find our simulations lie within the range of historically observed sugarcane and cotton yields from SPAM in Ethiopia (HarvestChoice, 2014). Again, any recommendations based on our modeling should only be made after obtaining more site-specific data for calibration and validation.

2.4 METHODS

In this study, we develop new reservoir operating policies for the SWAT model using non-linear (NL) release rules. We evaluate the performance of our release rules compared to existing reservoir operating rules in the SWAT model to see if we can better meet the needs of conflicting stakeholders in the Omo River Basin. For existing reservoir operations, we use the monthly target storage rule curve (RC) operations. We optimize reservoir operations for both RC and NL operations using Evolutionary Multi-Objective Direct Policy Search (EMODPS) so we can compare these operations at their respective peak performances.

2.4.1 Evolutionary Multi Objective Direct Policy Search

The EMODPS framework couples the Direct Policy Search (DPS) approach with Multi Objective Evolutionary Algorithms (MOEAs). EMODPS is a parameterization-simulation-optimization approach (Koutsoyiannis & Economou, 2003) that has been used to solve high-dimensional water resources and control problems; specifically, EMODPS has been successfully used to define closed-loop, flexible reservoir operating policies that best balance multiple, conflicting objectives (Giuliani et al., 2016b).

The EMODPS framework defines a reservoir operating policy within a family of func-

tions. The parameters of those functions are then optimized with respect to operating objectives, rather than optimizing the releases themselves. After an initial parameter set is defined, the system is simulated and performance is evaluated based on the operating objectives. The iterative search algorithms in MOEAs are then able to create and evolve a Pareto-approximate set of solutions over the problem's conflicting objectives through randomized mating, selection, and mutation operations.

2.4.2 Modifications to SWAT

Since existing reservoir operations in SWAT are limited and overly simplistic, we modify the source code of the reservoir module to provide an additional outflow simulation code that is capable of simulating non-linear operating policies optimized using EMODPS.

The modified source code reads optimized function parameters from user-defined text files in the `modparm` and `readres` modules, which are then passed to the reservoir module (`res`) and used to calculate daily releases using radial basis functions (RBFs). The RBFs determine release decisions as a function of multiple variables: the reservoir storage volumes across all reservoirs in the system at the beginning of the day and the day of the year. The source code is modified in order to pass this information to the RBFs. These updates to the source code allow the model to calculate daily releases using information about the system state.

2.4.3 Formulation of Objectives and Constraints

In order to evaluate system performance of our updated reservoir operations, we define five operating objectives and a constraint to capture the multiple and conflicting needs of different stakeholders in the basin: hydropower production, environmental protection, preservation of recession agriculture, sugarcane yield, cotton yield, and flood protection.

Hydropower. The hydropower objective, to be maximized, is calculated as the sum of the average annual hydropower production across the four power plants in the Omo River basin, to be maximized:

$$J^{hyd} = \frac{1}{H} \sum_{h=0}^{H-1} \sum_{i=1}^{N_y} G_{h+1}^{i} \qquad \text{with } i = GI, GII, GIII, K \tag{2.2}$$

where G_h is the daily hydroelectric power production in GWh, H is the number of time steps in the operating horizon (here, 13,879 days), and N_y is the number of hydropower producing dams (here, 4 dams). This objective captures the interest of the Ethiopian government.

Environment. This objective seeks to preserve natural flow conditions in the Omo River delta. It is computed as the daily average squared distance between the flow in the Omo River delta q_h^{delta} and the natural pattern q_h^{natOmo}, to be minimized:

$$J^{env} = \frac{1}{H} \sum_{h=0}^{H-1} \left(q_{h+1}^{natOmo} - q_{h+1}^{delta} \right)^2 \tag{2.3}$$

The historical pattern is calculated as a 30-day rolling average of the cyclostationary daily mean flows in the delta from an uncontrolled model run using weather inputs from 1989-2018 with an 8-year spin-up period from 1981-1988. This objective assumes that historical conditions are optimal for aquatic wildlife, grazing patterns, and overall environmental health in the Omo River delta.

Recession Agriculture. The recession agriculture objective is meant to preserve the annual flood pulse that indigenous tribes in the Lower Omo Valley rely on for their main source of food, and that the dams have historically dampened. It is calculated as the daily average squared distance between flow in the Lower Omo q_{h+1}^{LO} and a target artificial flood q_h^{AF}, to be minimized.

$$J^{rec} = \frac{1}{H}\sum_{h=0}^{H-1}\left(max\Big((q_h^{AF} - q_{h+1}^{LO}), 0\Big)\right)^2 \tag{2.4}$$

The target flood, q_h^{AF}, is zero for most of the year. The recession pattern starts on August 29 and linearly increases from 240 cms to a peak of 1200 cms on September 2. This target plateaus at 1,200 cms until September 11, and then decreases linearly until September 16 when it reaches 0 cms again.

Sugarcane Yield. The sugarcane objective is designed to capture the interests of the Kuraz Sugar Development Project, whose goal is to maximize sugarcane yields. This objective is calculated as the average annual sugarcane yield over the simulation horizon, to be maximized:

$$J^{sug} = \frac{1}{A}\sum_{a=0}^{A-1}\sum_{s=1}^{S} Y_a^s \tag{2.5}$$

where S is the number of sugarcane HRUs representing the Kuraz Sugar Development Project, A is the number of simulated years (here, 30), and Y_a^s is the annual yield in a given sugarcane HRU.

Cotton Yield. The cotton objective is designed to capture the interests of private agricultural holdings, which will likely primarily grow cotton (Carr, 2017; Hodbod et al., 2019). This objective is calculated as the average annual cotton yield over the simulation horizon, to be maximized:

$$J^{cot} = \frac{1}{A}\sum_{a=0}^{A-1}\sum_{c=1}^{C} Y_a^c \tag{2.6}$$

where C is the number of cotton HRUs representing private agricultural holdings in the Lower Omo Valley and Y_a^c is the annual cotton yield in a given HRU.

Flood Constraint. This optimization is subject to a single constraint, which specifies

flows in the Lower Omo Valley should not exceed their historical uncontrolled maximum:

$$\max\left(q_{max}^{LO} - 3290, 0\right) = 0 \tag{2.7}$$

where q_{max}^{LO} is the maximum flow in the Lower Omo Valley over the simulation horizon and 3,290 cms is the maximum historical flow observed in an uncontrolled model run. This objective aims to mitigate flood concerns in the basin. While indigenous tribes rely on a moderate flood pulse, large floods have damaged their crops and dwellings and even resulted in loss of life (EEPCO, 2008). This was documented in August 2006, when a flood flows that peaked somewhere between 3,500 and 4,000 cms caused the death of hundreds of people and displaced thousands more. We include this constraint so that we do not design policies that could cause such destructive flood pulses downstream.

2.4.4 Formulation of Operating Policies

The existing RC operations are equivalent to piecewise linear functions for each reservoir in the system. Each reservoir's policy is defined by 13 parameters: a target storage value for each month (`STARG`) and the number of days it takes to reach target storage (`NDTARGR`), which is constant across all months, resulting in a total of 39 parameters to define these operating policies. Existing RC policies are not fully state-aware, as each reservoir's release decision is based only on its own storage level and the month but does not consider the storage at the other two reservoirs.

The NL operating policies are defined as Gaussian RBFs, which Giuliani et al. (2016b) show to be more effective in solving multi-objective policy design problems than other universal approximators, like Artificial Neural Networks (ANNs). Operating policies defined by RBFs prescribe daily releases, u_t^k, normalized on [0,1] from the k-th reservoir at time t as a function of B time-varying inputs, v_t, normalized on [0,1], and an optimized

base release for the reservoir, normalized on [0,1], a_k:

$$u_t^k = a_k + \sum_{i=1}^{N} w_{i,k} \exp\left(\sum_{j=i}^{B} \frac{\left((v_t)_j - c_{i,j}\right)^2}{b_{i,j}^2} \right). \tag{2.8}$$

Here, N is the total number of RBFs, $w_{i,k}$ is the weight of the i-th RBF, and v_t is a vector of the reservoir volumes at time t normalized over [0,1] and a cyclic representation of time. B is the number of policy inputs, and (c_i, b_i) are the B-dimensional center and radius vectors of the i-th RBF, respectively. The weights do not sum to 1, and therefore do not represent a convex combination.

The true release realized by the end of day t, r_{t+1}^k, is determined by subjecting the prescribed release to physical and minimum environmental flow (MEF) constraints. These ensure the releases meet MEF requirements when feasible, outflows do not exceed the maximum capacity of turbines, and the reservoir does not exceed its capacity. The MEFs are 1.3 cms for Gibe I, 70 cms for Gibe III, and 25 cms for Koysha (Badagliacca & Spinelli, 2018; MDI Consulting Engineers, 2016).

The parameter vector $\theta = [c_{i,j}, b_{i,j}, w_{i,k}]$ with $i = 1...N$, $j = 1...B$, and $k = 1...K$ is optimized using the Borg Multi-Objective Evolutionary Algorithm. Here, N = 9 RBFs, $K = 3$ reservoirs (Gibe I, Gibe III, and Koysha all have storage reservoirs), and B = 5 inputs: the storage at each of the three reservoirs and a cyclic representation of time captured by $\frac{1}{2}[\sin\left((2\pi t)/365\right)+1]$ and $\frac{1}{2}[\cos\left((2\pi t)/365\right)+1]$. The total number of optimized parameters in each of the operating policies is $K + N(2B + K) = 120$ parameters.

2.4.5 Multiobjective Optimization

In this study, we use the Borg Multi-Objective Evolutionary Algorithm with the EMODPS framework (Hadka & Reed, 2013). The Borg MOEA, which includes epsilon-dominance archiving, operators that can flag search stagnation, randomized restarts to escape lo-

cal optima, and adaptive selection of search operators, is highly robust in solving multi-objective optimization problems, and has been shown to perform as well or better than other MOEAs across a wide range of problem formulations (Hadka & Reed, 2013).

In addition to the 39 reservoir operating parameters for RC operations and 120 reservoir operating parameters for NL operations, we also optimize 5 irrigation parameters: the water stress threshold that triggers irrigation (`AUTO_WSTRS`) and the amount of irrigation water applied each time the auto irrigation is triggered (`IRR_MX`) for sugarcane and cotton, as well as a single value of the water stress identifier (`WSTRS_ID`), which decides whether irrigation is triggered by plant water demand or soil water content, which we hold constant for both cotton and sugarcane. This brings the total number of decision variables to 44 and 125 for RC and NL, respectively.

For both existing RC and updated NL policy designs, the operating policy is defined within a class of functions p_θ (piecewise linear storage targets for RC and RBFs for NL) and Borg searches for the best parameterization, θ^*, for the given class:

$$p_\theta^* = argmin_{p_\theta}(\bar{J}) \tag{2.9}$$

where

$$\bar{J} = |-J^{hyd}, J^{env}, J^{rec}, -J^{sug}, -J^{cot}|. \tag{2.10}$$

Each element of $\bar{J}$ is defined in Section 2.3.3. The outcome of the optimization is a set of non-dominated solutions, called the Pareto-approximate set, in which no solution outperforms another on all objectives.

We use a Multimaster parallelization of the Borg MOEA (Hadka & Reed, 2015) with two masters to optimize RC and NL operating policies on Rivanna, the University of

Virginia's High Performance (HPC) computing cluster. A scaling analysis indicates that 240 cores yields optimal performance rather than Rivanna's maximum of 1,000 cores per job. While the Borg algorithm scales well (Hadka & Reed, 2015), the large number of input files required by the SWAT model degrade system performance and slows optimization as more copies of the model are required.

We compare RC and NL performance after 190,000 function evaluations, which is the maximum number of function evaluations (NFE) that both problem formulations could achieve in 72 hours, the computation time limit on Rivanna. Visual inspection of hypervolume indicates that the search was adequate for both problem formulations, as hypervolume had leveled out, indicating that we had reached a point of diminishing returns for RC and NL after 190,000 NFE (see Figure 2.3 in Section 2.5). We thin the Pareto approximation sets by re-sorting them with larger epsilon values (Table A.3) to yield a reduced but representative set of operating policies for both RC and NL policies.

2.4.6 Performance Evaluation

We first compare the performance of RC and NL policies on each objective under historical climate conditions to which they were optimized. To assess the adaptivity of these respective policy designs, we then compare the performance of RC and NL policies under alternative climate scenarios. We use daily projections from 48 General Circulation Models (GCMs) in the Coupled Model Intercomparison Project 5 (CMIP5) multimodel ensemble with a single set of initial conditions across all four representative concentration pathways (RCPs). A list of all climate projections used in the study is provided in Table A.2.

We bias correct daily CMIP5 estimates of precipitation, minimum temperature, and maximum temperature to daily 0.05° CHIRPS precipitation data and resampled daily 0.1°

Copernicus ERA-5 2m air temperature data. The downscaled data is then aggregated to the sub-basin level using the same approach described in Section 2.3.2 for the historical data. We use a variation of the modified equidistant cumulative distribution function matching (EDCDFm) algorithm for bias correction (Li et al., 2010; Pierce et al., 2015) used by Quinn et al. (2018) in the Red River Basin in Vietnam. This variation of EDCDFm applies the technique to daily temperature and precipitation anomalies, rather than absolute values. This preserves model-predicted median change while avoiding multiplicative instabilities associated with EDCDFm of daily precipitation data, since anomalies can be either multiplicative or additive. We only apply EDCDFm over wet days when bias correcting precipitation to allow a model-predicted increase in the number of wet days. Finally, we apply a method that better balances the correction of extremes and the annual cycle than the original technique. Bias correction applied over a small, moving time window will correct the annual cycle, but may not accurately correct extremes. However, bias correction applied without a moving time window will correct extremes but not the annual cycle. We therefore bias correct both with and without a 31-day moving window and then bias correct the values from the 31-day moving window using those from the bias correction without the moving window to more accurately capture the behavior of both extremes and the annual cycle.

We then statistically downscale the debiased CMIP5 temperature and precipitation projections using a variation of the constructed analog approach (CAA) developed by Pierce et al. (2014), a method termed Constructed Analogs with Single Anomaly Analog (CASAA). CASAA uses anomalies for downscaling both temperature and precipitation, instead of using anomalies for downscaling temperature and absolute values for downscaling precipitation, as this improves the performance of precipitation downscaling. The updates also help preserve the high-resolution wet-dry spatial pattern compared to CAA.

A more detailed description of the bias correction and spatial downscaling can be found in the supporting information to Quinn et al. (2018).

Finally, we define new temperature and precipitation inputs from each climate projection and run SWAT using both RC and NL policy designs. Each of the five objective values are calculated over a 30-year horizon at mid-century (2040-2069) or at the end of the century (2070-2099) for the alternative management strategies.

2.5 RESULTS AND DISCUSSION

2.5.1 Performance Evaluation Across Objectives

We first compare the performance of the RC and NL policies in terms of hypervolume, the n-dimensional volume of objective space dominated by a Pareto approximate set. We express the hypervolume of the RC and NL Pareto approximation sets throughout their search as a fraction of the hypervolume of the best known approximation of the Pareto set computed with respect to a reference point (Figure 2.3a). The best known approximation of the Pareto set is found by performing a non-dominated sort of the final policies from the RC and NL Pareto approximation sets. The larger the hypervolume, the better the solutions in the Pareto approximation set.

In order to track the performance of EMODPS over the course of optimization, we examine the hypervolume at every thousandth function evaluation (Figure 2.3b). Hypervolume for both NL and RC levels out by the end of the search, which indicates that optimizaton of both policy designs was able to converge. However, NL policies have a higher hypervolume for all NFE. This means that the updated policies perform better than the existing RC policies in SWAT throughout the optimization process, despite the higher number of decision variables included in the NL policy design.

We next compare the individual policies from these Pareto sets. To yield a reduced

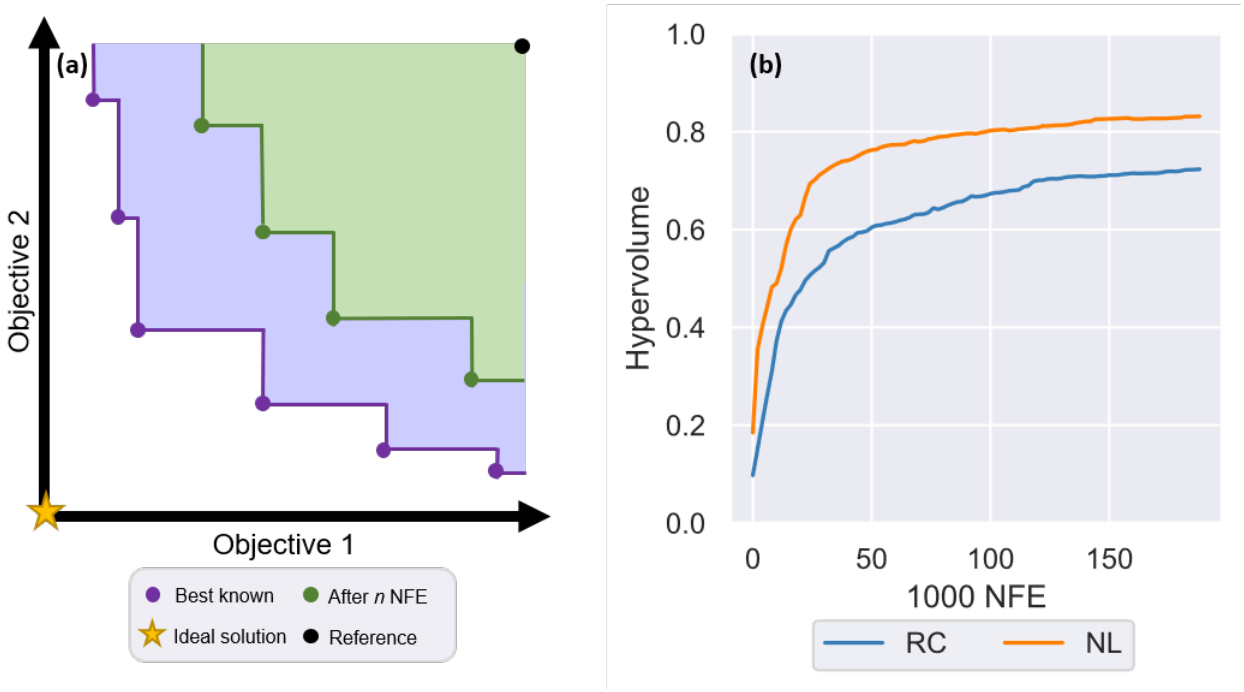

Figure 2.3: (a) Depiction of hypervolume calculation. (b) Progression of hypervolume for RC and NL relative to their combined Pareto set over the course of multiobjective optimization. NFE = Number of Function Evaluations.

but representative set of operating policies for both RC and NL formulations, we thin the Pareto approximation sets by re-sorting them with larger epsilon values. From the thinned sets, we see that optimizing reservoir operations with the nonlinear operating rules results in more Pareto-optimal policies than optimizing existing rule curve policies in SWAT: there are 98 NL Pareto-optimal solutions compared to 59 RC solutions (Table 2.3). We then combine the individual Pareto sets for RC and NL policies into a single set of Pareto-optimal reservoir operating policies. We find that the updated SWAT policies tend to dominate policies designed with SWAT's existing reservoir operations, meaning that the NL policies tend to perform as well or better across all objectives compared to the RC policies, since 77% of the NL policies make it into the combined Pareto set (75 policies) while only 41% of the RC policies do (24 policies).

Table 2.3: Number of policies in individual and combined Pareto approximation sets.

	RC	NL
Individual	59	98
Combined	24	75

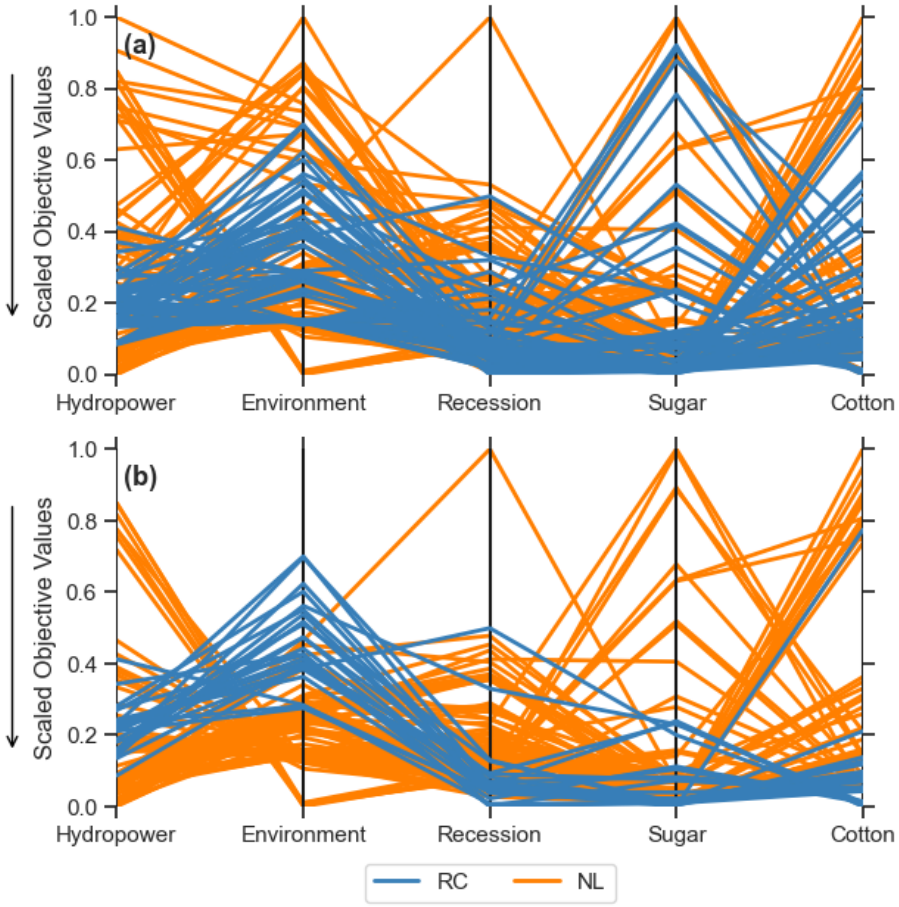

Figure 2.4: Policy performance of (a) all RC and NL policies in their individual Pareto sets and (b) in their combined Pareto set.

The performance of these policies across our five operating objectives is visualized in a parallel axis plot (Figure 2.4). In parallel axis plots, each vertical axis represents policy

performance on each objective of interest and each line represents a single reservoir operating policy, crossing the axes at its objective values. Here, each axis is oriented such that favorable performance is down. When lines intersect between the vertical axes, this indicates trade-offs between the corresponding objectives of those policies. As can be seen in Figure 2.4, strong policy performance on one objective often comes at the expense of one or more other objectives. For example, policies that perform best on the environmental flows objective tend to suffer on hydropower performance and vice versa.

Figure 2.4a shows the performance of all RC and NL policies in their individual Pareto sets while Figure 2.4b shows the performance of just policies in the combined Pareto set. The NL policies tend to far outperform RC policies on hydropower production and environmental flows objectives while still maintaining strong performance on the recession, sugar, and cotton objectives. The RC policies, on the other hand, struggle to balance these five objectives. The RC policies have particularly poor performance compared to NL policies on the environmental flows objective, failing to produce operations that can mimic the pre-dam flow regime that supports ecological health in the Omo delta.

2.5.2 Performance Evaluation on Individual Objectives

From each formulation's individual Pareto set, we select the five policies that perform best on each objective to analyze more deeply. The performance of these policies on each objective is provided in Tables A.4 and A.5.

Examining average daily reservoir storage levels allows us to see how different reservoir operations enable the solutions to attain near-optimal performance on particular objectives. Average daily reservoir storage levels over the simulation horizon for RC policies are shown in Figure 2.5a for Gibe III and 2.5c for Koysha, the two largest reservoirs. Storage levels at Gibe III tend to stay slightly higher for the best hydropower RC policy, but

otherwise, there are no clear trends across policies. Similarly, storage levels are nearly the same across policies for Koysha, with only the best sugar policy distinguishing itself with a dip in reservoir levels in April to provide water for irrigation. However, this results in a spike in streamflow downstream at the same time since not all of this water was abstracted for irrigation (Figure 2.6a,c). A longer search time during optimization could likely find a policy that can provide adequate downstream flows for irrigation with a less dramatic release pattern. For example, the best policy for sugarcane with the NL policy design has the highest average downstream flows during the dry season so that water is available for irrigation as needed without a dramatic pulse and while maintaining fairly high reservoir levels at Koysha (Figure 2.5 and 2.6 b,d).

Differences across policies are much more significant for the new NL policies (Figure 2.5b for Gibe III and Figure 2.5d for Koysha). For the NL policies, the best policy for hydropower maintains notably higher reservoir levels at both Gibe III and Koysha to create a high head differential for more power production. The best policies for other objectives favor releasing more water downstream, so reservoir levels are much lower. The best policy for environmental flows has low levels at Koysha on average, likely because it needs to release a lot of water from this reservoir to hit daily downstream flow targets. However, this same policy maintains the second highest reservoir levels on average at Gibe III, the reservoir directly upstream from Koysha, showing how it coordinates operations between the two to balance conflicting objectives. The best policies for recession agriculture, sugarcane, and cotton coordinate operations in the opposite manner, maintaining fairly low levels at Gibe III and fairly high levels at Koysha. These policies generally need more water on demand, either to meet the flood recession target or to supply water to crops during dry periods, so keeping reservoir levels high at Koysha ensures water is available to deliver downstream as needed. The best policy for cotton rises around June in prepa-

ration for when cotton starts to grow in July. While the levels at Koysha stay high for the recession, sugarcane, and cotton objectives, reservoir levels at Gibe III tend to stay fairly low. This could be a mechanism to protect against unnecessarily high releases; if the reservoir levels at Gibe III are low, this reservoir can capture extra inflow so that Koysha levels can stay high without risk of inundating downstream areas. This demonstrates the ability of the updated reservoir operations to coordinate release behavior between reservoirs.

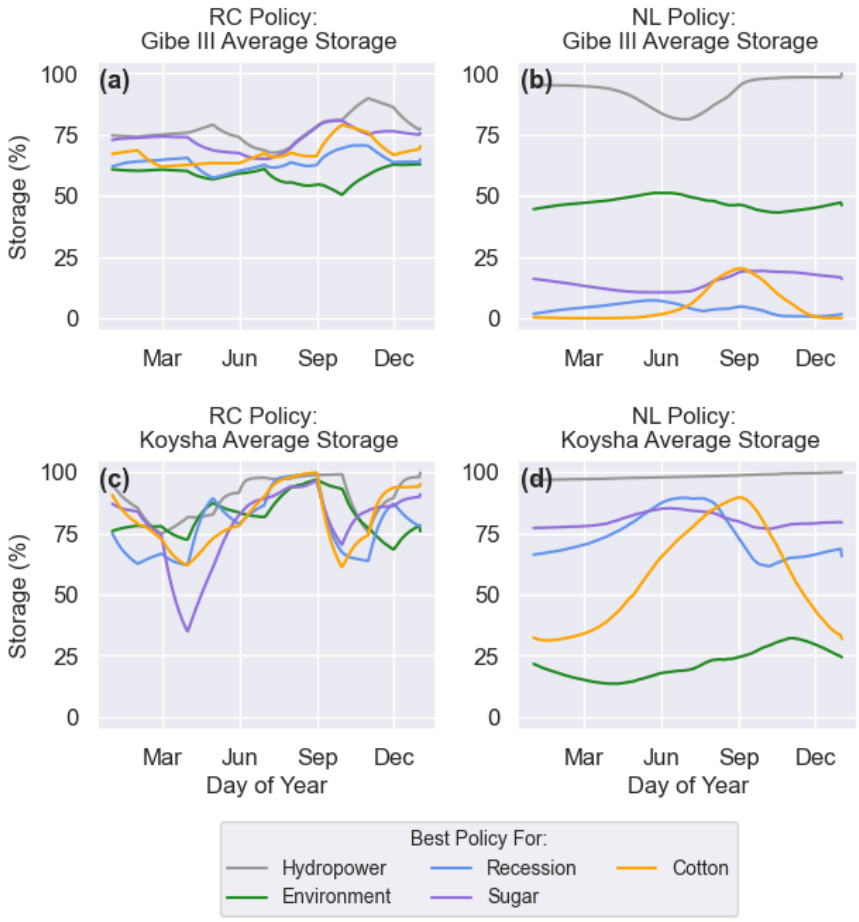

Figure 2.5: Average daily reservoir storage levels as a percent of operational capacity at Gibe III and Koysha for RC and NL policies that perform best on each of the five objectives.

It is also informative to visualize how alternative reservoir release policy designs im-

pact downstream flows. Figure 2.6a-b shows flows in the Omo River Valley, where we aim to replicate a flood pulse from late August to mid-September. Figure 2.6c-d shows flows in the Omo delta from different policy designs compared to the historical pattern. Once again, it is difficult to parse out trends in the RC policies other than a spike in the releases for sugar in April. Additionally, while the flows generally follow the natural hydrograph, they are far more erratic due to the monthly storage targeting.

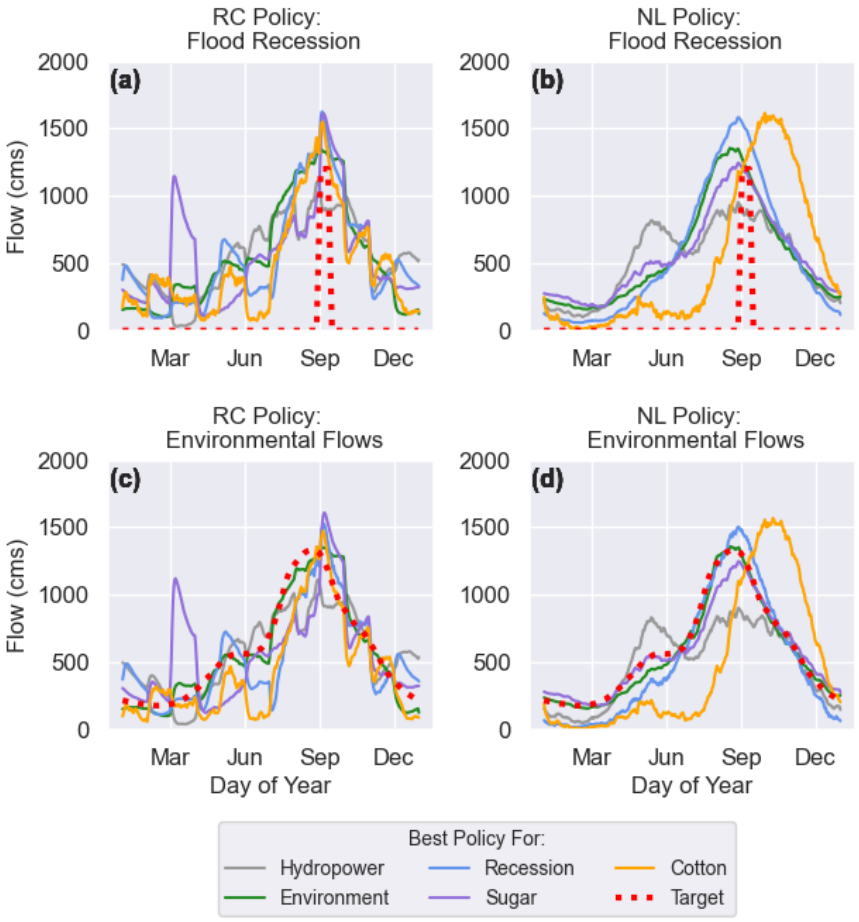

Figure 2.6: Average daily flows downstream of the dams for RC and NL policies.

For the NL formulation, the best policies for environmental flows, recession agriculture and sugar are able to mimic this behavior much more smoothly. The best policy

for hydropower dampens peak flows in the Omo River Valley and delta since it keeps the reservoir levels so high, failing to meet historical targets. This reduces intra-annual variability, with higher flows in May and lower flows in September. The best policy for recession agriculture reaches a peak slightly after the environmental flows target in order to meet the timing of an ideal flood pulse. The best policy for cotton dampens flows during the dry season and shifts the seasonality of flows so that the peak arrives in October to November.

2.5.3 Performance Evaluation under Climate Change

As a final comparison between the existing SWAT reservoir operations and the updated policy design, we track how policies from the two operating strategies perform in SWAT simulations using weather inputs from 48 downscaled climate projections. This assesses how robust the policies are to conditions outside of those to which they were optimized, but under which they may need to operate in the future. We plot the performance of each policy in mid- and late century for each objective and climate scenario in Figure 2.7. To illustrate if water infrastructure development is exacerbating or mitigating the impact of climate change on different stakeholders in the Omo River basin, we also plot the performance of an uncontrolled scenario (i.e. no reservoirs and no irrigation) under each climate scenario in black as a reference for how the system would perform without the reservoirs.

Similar to Figure 2.4, each line in Figure 2.7 represents a different operating policy, but the x-axis here corresponds to different climate projections. The climate projections are sorted from lowest to highest mean inflow for the hydropower, environmental flows and recession agriculture objectives and from lowest to highest mean temperature for sugarcane and cotton yields, as these climate characteristics are most predictive of their per-

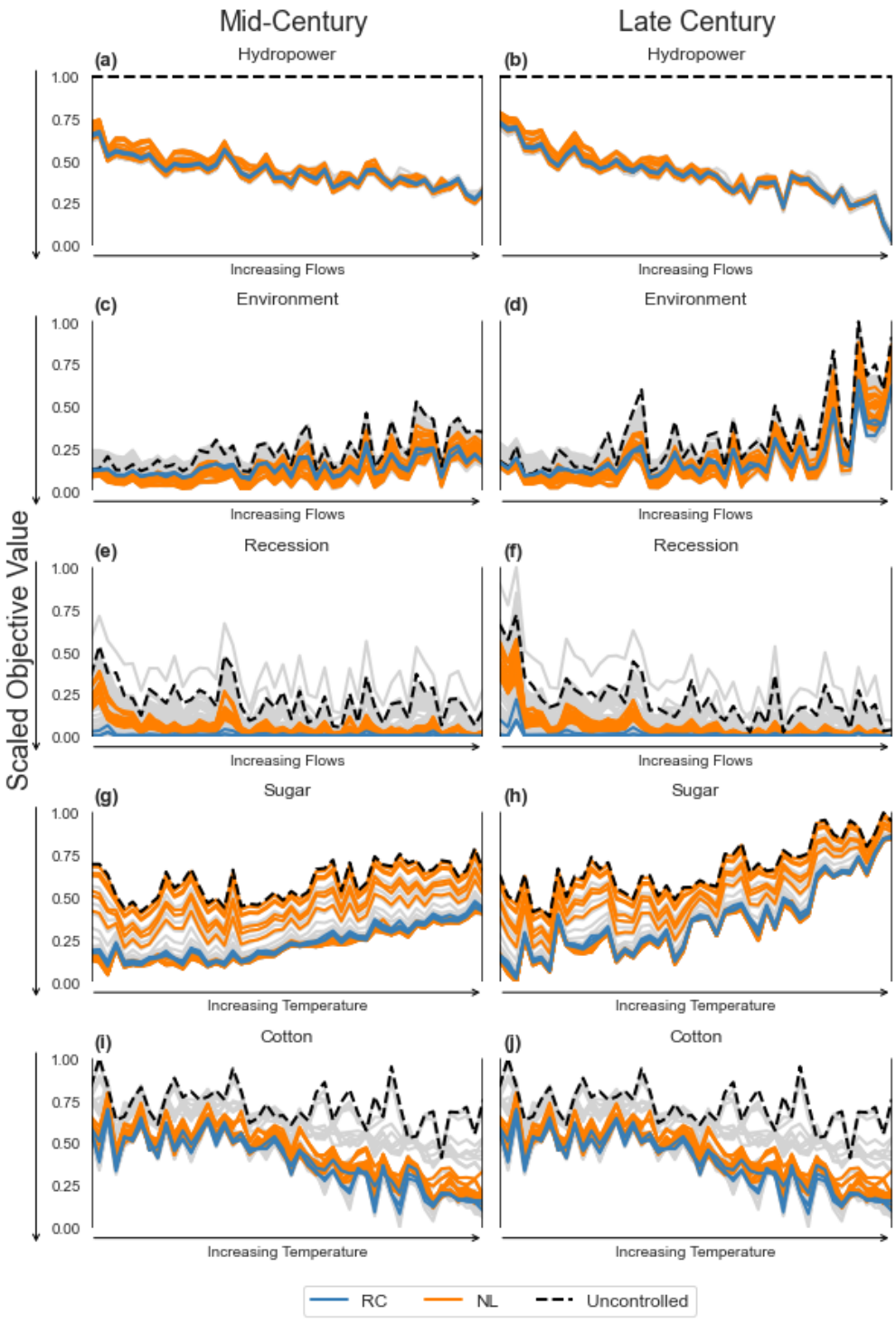

Figure 2.7: Performance of RC and NL policies for 48 climate projections. Policies that do not perform better than an uncontrolled simulation across all objectives and all projections are greyed out.

formance. Each objective is oriented such that the favorable direction is down. As such, we see that hydropower and recession agriculture performance improve with higher inflows, while environmental flows degrade, and sugarcane yields decrease with higher temperature, while cotton yields increase.

To compare the robustness of different operating strategies, we define policies as "robust" if they perform better than the uncontrolled scenarios across all objectives and all projections in both mid- and late century. 20 NL policies from the combined Pareto set meet these criteria, while just 3 of the RC policies do. Policies that do not meet these criteria have been grayed out. Comparing the 20 robust NL policies and 3 robust RC policies, we see the best NL policies for hydropower and environmental flows tend to outperform the RC policies across all climate projections on these objectives. However, the RC policies tend to outperform the NL policies across all projections on recession agriculture and perform comparably to the best NL policies on sugar cane and cotton yields. This is because the only RC policies that perform robustly across projections favor those objectives (Figure 2.8).

To understand why so few RC policies are able to balance the five conflicting system objectives in possible climate futures compared to the NL policies, we investigate how the NL and RC operating rules adapt in response to different climate conditions. For this comparison, we choose a representative compromise solution among the robust NL and RC policies. The historical performance of these compromise policies is shown in Figure 2.8a, along with the other policies that meet our robustness metric. The non-robust operating policies are grayed out. Figure 2.8b-e illustrate the operating behavior of these two policies under each climate projection. Each line represents the average daily reservoir storage in each climate projection. The lines are colored by the average flow in the Omo Delta in that projection's uncontrolled scenario as a proxy for how wet or dry that climate

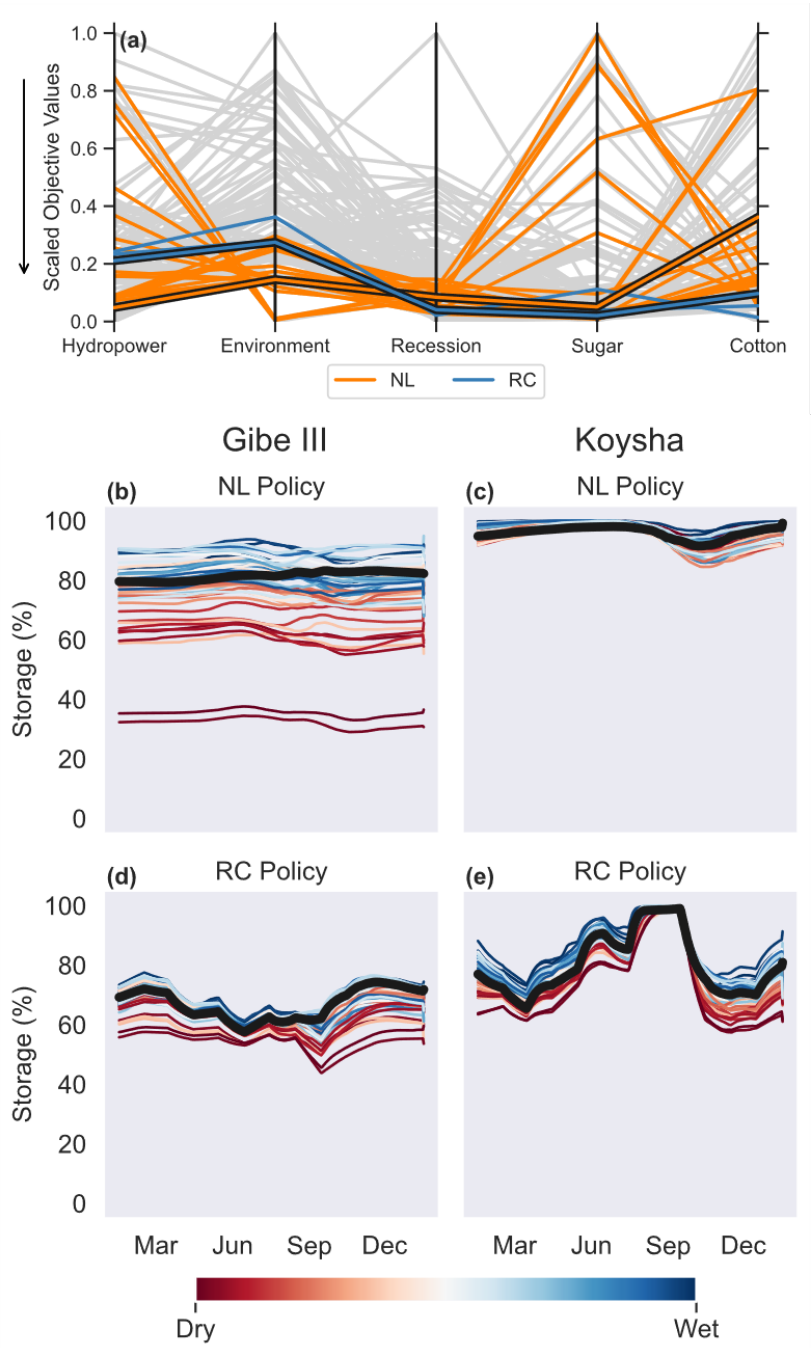

Figure 2.8: (a) Historical performance of robust RC and NL policies. Compromise RC and NL policies are outlined in black. (b-e) Reservoir behavior of compromise policies showing the average daily reservoir storage for the NL compromise policy at (b) Gibe III and (c) Koysha and for the RC compromise policy at (d) Gibe III and (e) Koysha. The historical average levels for each policy are shown in black.

projection is. The average daily level of the operating policies during the historical record is shown with a thick black line.

We see reservoir levels at Gibe III drop in dry projections or rise slightly in wet projections compared to the historical average level for the NL policy so that Koysha levels can stay consistently high. This ensures enough water is released from Gibe III and available in Koysha to release downstream for environmental flows and recession agriculture. In contrast, the RC policies tend to mirror levels at both reservoirs, dropping or rising slightly depending on the projection; there is no adaptive coordination, just failure to meet target levels when supply is higher or lower. This highlights the benefits of the NL policies' fully state-aware control rule, which allows it to adapt how it coordinates synergistic releases across reservoirs. These features likely help NL policies better balance downstream flow objectives across a wider range of future scenarios compared to RC policies.

2.6 CONCLUSIONS

This study uses the multireservoir Omo River system in Ethiopia to demonstrate the power of modeling closed-loop, nonlinear, and state-aware reservoir operating policies in a SWAT model. The existing reservoir operations in SWAT fail to produce solutions that balance the needs of all stakeholders in the basin while the updated operations allow for more flexible and adaptive policies that can produce positive outcomes for economic, agricultural, social, and ecological objectives. Furthermore, far more nonlinear policies out-perform uncontrolled conditions under possible climate futures than the existing RC policies, highlighting the importance of adaptability in reservoir operations in meeting conflicting water demands.

These benefits extend beyond the Omo River basin. Using EMODPS to optimize non-

linear operating policies in SWAT allows us to capitalize on SWAT's ability to model both natural and human components of river systems better than traditional reservoir models such as HEC-ResSim (USACE, 2007) and Riverware (Zagona et al., 2001). For example, we take advantage of SWAT's ability to simulate crop growth in order to directly optimize crop yields rather than relying on indirect objectives like minimizing water supply deficit. Furthermore, simulating these policies in SWAT allows for a more accurate climate impact assessment than traditional reservoir simulation models that take streamflows as input, as the rainfall-runoff relationship is modeled explicitly in SWAT. Of course, reservoir operations are just one piece of the larger coupled natural human system dynamics between water and land management decisions and ecological health, and climate conditions are only one possible exogenous influence on their dynamics. SWAT facilitates more integrated assessments of how changes in multiple drivers beyond climate, including changes in land use and land management, influence vulnerabilities. Furthermore, future work can explore how additional management decisions such as fertilizer application can be optimized in conjunction with alternative reservoir operating strategies.

As the climate changes, the government, private agricultural stakeholders, and indigenous people will all need to make adaptation decisions in how they manage land and water resources, and more sophisticated reservoir operations could ease that adaptation. For example, sugarcane and cotton plantations will need to decide when and how to apply fertilizer and irrigation or if they want to invest in soil conservation projects; and indigenous people will need to decide which crops to plant in what quantities and whether or not they should migrate. These decisions will all depend on how the government chooses to operate dams, and whether or not they purchase more land for irrigable agriculture development. The advanced reservoir operations in SWAT allow us to model a suite of optimized release rules in tandem with these possible changes in system dy-

namics to understand how changing climate and human decisions impact economic and socio-ecological outcomes, and to inform favorable adaptation.

CHAPTER 3

Rethinking reservoirs: how smart operations can yield win-win climate adaptation outcomes

3.1 ABSTRACT

Climate change is projected to increase the intensity and frequency of extremes in river basins around the world. Robust and adaptive reservoir management will be essential in buffering against droughts, providing flood protection, and balancing socio-ecological tradeoffs as precipitation patterns change. This study uses the advanced reservoir module in SWAT with the model's existing ability to simulate climate change scenarios to identify robust policies that mitigate high and low flows in the Omo River basin of Ethiopia. We identify policies that are able to mitigate the impact of climate change on extreme flow events while still balancing economic, agricultural, social, and ecological outcomes. We find that these robust policies exhibit tradeoffs between preserving the distribution of historical high or low flows, but that compromise solutions exist that can yield win-win climate adaptation outcomes.

3.2 INTRODUCTION

Climate change is expected to intensity the hydrologic cycle, and such behavior is already being observed in river basins around the world (Huntington, 2006). Changes in precipitation patterns, soil moisture content and runoff, and increasing frequency and intensity of extreme rainfall events are causing more extreme floods and droughts (Boulange et al., 2021; Bates et al., 2008). Water resources managers have often relied on reservoirs to mitigate these conflicting risks while still meeting other economic, agricultural, social, and ecological river basin demands (Hall et al., 2014). Consequently, climate adaptation

research has largely focused on mitigating impacts by increasing infrastructure development, such as building new dams, restoring or increasing the size of old dams, or transferring water between catchments to balance supplies during drought (Watts et al., 2011; Zeff et al., 2016; Poff et al., 2016).

However, dam planning, construction, and maintenance are all expensive and time-intensive, often costing billions of dollars over many years to complete. More concerningly, dams may displace communities and disrupt ecological processes, making them both socially and politically controversial (Ehsani et al., 2017; IUCN Water, 2019). Recognizing these consequences, recent research has focused on siting, sizing and operating dams to mitigate socio-ecological impacts (Sabo et al., 2017; Wild et al., 2019; Schmitt et al., 2018). However, these studies have not considered whether these designs would still be sufficient under climate change. Altered precipitation patterns could reduce river flows, decreasing the projected economic benefits from hydropower production, stranding over-designed assets at the expense of displaced communities and the ecology (Cole et al., 2014). On the flip side, under-designed infrastructure could lead to increased risks of floods or droughts (Lumbroso et al., 2015).

However, many of these impacts will be felt in absence of infrastructure development as well. In understanding the vulnerability of reservoir systems to climate change, it is important to consider whether the infrastructure is mitigating or exacerbating those impacts. Do win-win climate adaptation strategies exist that not only reduce social vulnerabilities to floods and droughts, but also mitigate ecological impacts to these changing extremes?

In this study, we leverage the advancements made to SWAT's reservoir module in Chapter 2 to test if smart operating policies can continue to reduce socio-ecological trade-offs in the Omo River basin while mitigating the impact of climate change on flow ex-

tremes. While we designed these policies so as not to exceed historical maximum flows and to meet minimum environmental flow thresholds downstream of the dams, changing climatic stressors may force these conditions to be violated, which could create a new set of challenges in the basin. We perform a climate risk assessment to determine whether water infrastructure development mitigates or exacerbates the impact of climate change on floods and droughts. We find some tradeoffs in the benefits of policies that best mitigate extreme high vs. low flows, but also identify win-win compromise policies that can balance the consequences of both while maintaining socio-economic and ecological benefits that would be unattainable without infrastructure development. We then compare and contrast how these policies achieve stable outcomes under a changing climate, highlighting the benefits of our coordinated, adaptive operations.

3.3 METHODS

In Chapter 2, we demonstrated that NL operating policies yield better objective value performance for a range of stakeholders under climate change than RC policies because they can adapt to system changes. In this chapter, we explore how NL policies optimized in Chapter 2 perform under changing wet and dry extremes. The goal is to see if these policies not only reduce the socio-ecological tradeoffs of reservoir development, but can also provide win-win climate adaptation strategies that mitigate ecological impacts of climate change while providing additional social benefits. We use the same calibrated SWAT model of the Omo River basin, system objectives, and downscaled climate projections as described in Chapter 2.

3.3.1 Identification of Annual Extremes

We start by defining our metrics for wet and dry extremes so we can discern how optimized reservoir operating policies mitigate or exacerbate these conditions.

We define wet extremes as the time series of annual maximum daily flows in the Omo River delta, which create an annual maxima series (AMS). Annual maxima series are used in flood frequency analysis to aid flood management, reservoir planning, and irrigation scheduling (Tiwari et al., 2017).

We do not want to simply define dry extremes as the annual minimum daily flow, since one day of low flows is not necessarily detrimental to the system. We therefore define dry extremes as the annual minimum seven-day flow series (7QS) in order to capture both persistence and severity. Seven-day low flows can be used to define environmental droughts such as the most commonly used low flow index in the United States: the seven-day, ten-year low flow, or 7Q10, defined as the annual minimum seven-day low flow that occurs, on average, once every ten years (Riggs, 1980).

We estimate AMS and 7QS time series in the Omo River delta from SWAT simulations under a historical uncontrolled scenario, as well as future uncontrolled scenarios from the 48 downscaled climate projections. This allows us to assess how ecological low flow and flood risks might change in the future in absence of adaptation. We repeat this using the optimized nonlinear reservoir operating policies from Chapter 2 to see if different operating rules exacerbate or mitigate these changing vulnerabilities.

3.3.2 Statistical Analyses

We compare the distributions of historical and future AMS and 7QS time series using the DTS test. The DTS test uses empirical cumulative distribution functions (ECDFs) to test the hypothesis that two samples come from the same distribution using a weighted

Wasserstein distance, the minimum distance you'd have to move one distribution to be the same as the other (Dowd, 2020). The weighting is inversely proportional to the predicted variance of the combined sample's ECDF at each point. Dowd (2020) shows the DTS test to be more powerful than most commonly used hypothesis tests between distributions, including the Kolmogorov-Smirnov test that has been used in the hydrology literature to assess whether human influences have changed the natural flow regime (Kroll et al., 2015).

For each of the 97 Pareto-optimal operating policies and the uncontrolled scenario, we use the DTS test to see if the distributions of the AMS and 7QS in each of the climate projections are statistically the same as the historical uncontrolled scenario (1989-2018) at mid- (2040-2069) and late century (2070-2099). For each policy and the uncontrolled scenario, we then calculate the percent of projections in which that policy's distributions of high and low flows are statistically the same as under the historical uncontrolled scenario at a 95% confidence level ($p > 0.05$). This helps us identify which policies are mitigating or exacerbating the effects of climate change on extreme high and low flows compared to the uncontrolled scenario.

In each projection, we also test whether or not there is a monotonic trend in the 7QS and AMS time series for each policy and the uncontrolled scenario. Operating policies that reduce the number of projections in which these time series exhibit a monotonic trend compared to the uncontrolled scenario enable favorable climate adaptation. We use the non-parametric Mann-Kendall trend test for this analysis (Mann, 1945; Kendall, 1948)

3.4 RESULTS AND DISCUSSION

3.4.1 Performance Evaluation on Wet and Dry Extremes

The historical performance of optimized reservoir operating policies is plotted on a parallel axis plot in Figure 3.1a. Policies are colored by their performance on the environmental flows objective, with green policies performing the best and yellow policies performing the worst. Four policies are outlined for their robustness to climate change on different performance metrics. In the previous chapter, we defined robust policies as those that were found to outperform an uncontrolled scenario on all objectives across all climate projections. While balancing economic, social, and ecological outcomes is essential, it is also important to consider how these alternative operating policies will handle extreme events, which are only projected to intensify under climate change.

In this chapter, we therefore consider three additional robustness metrics that captures a policy's performance in mitigating extremes under a range of conditions. All metrics are domain satisficing criteria quantifying the percent of climate projections in which some minimum performance threshold is met (Starr, 1963; Schneller & Sphicas, 1983). Here we define three minimum performance thresholds: no statistically significant difference in the distribution of 1) 7QS, 2) AMS, or 3) Both 7QS and AMS compared to the historical uncontrolled conditions (HUC). Operating policies with a higher satisficing metric than projected uncontrolled conditions (PUC) tend to mitigate the impacts of climate change on extremes, whereas operating policies with a lower satisficing metric may exacerbate the effects of climate change.

Figure 3.1b-d shows the satisficing metric of all operating policies at mid-century on (b) low flows, (c) high flows, or (d) both low and high flows (the same graph at late century is shown in Appendix Figure A.2). Policies are sorted within each panel from those

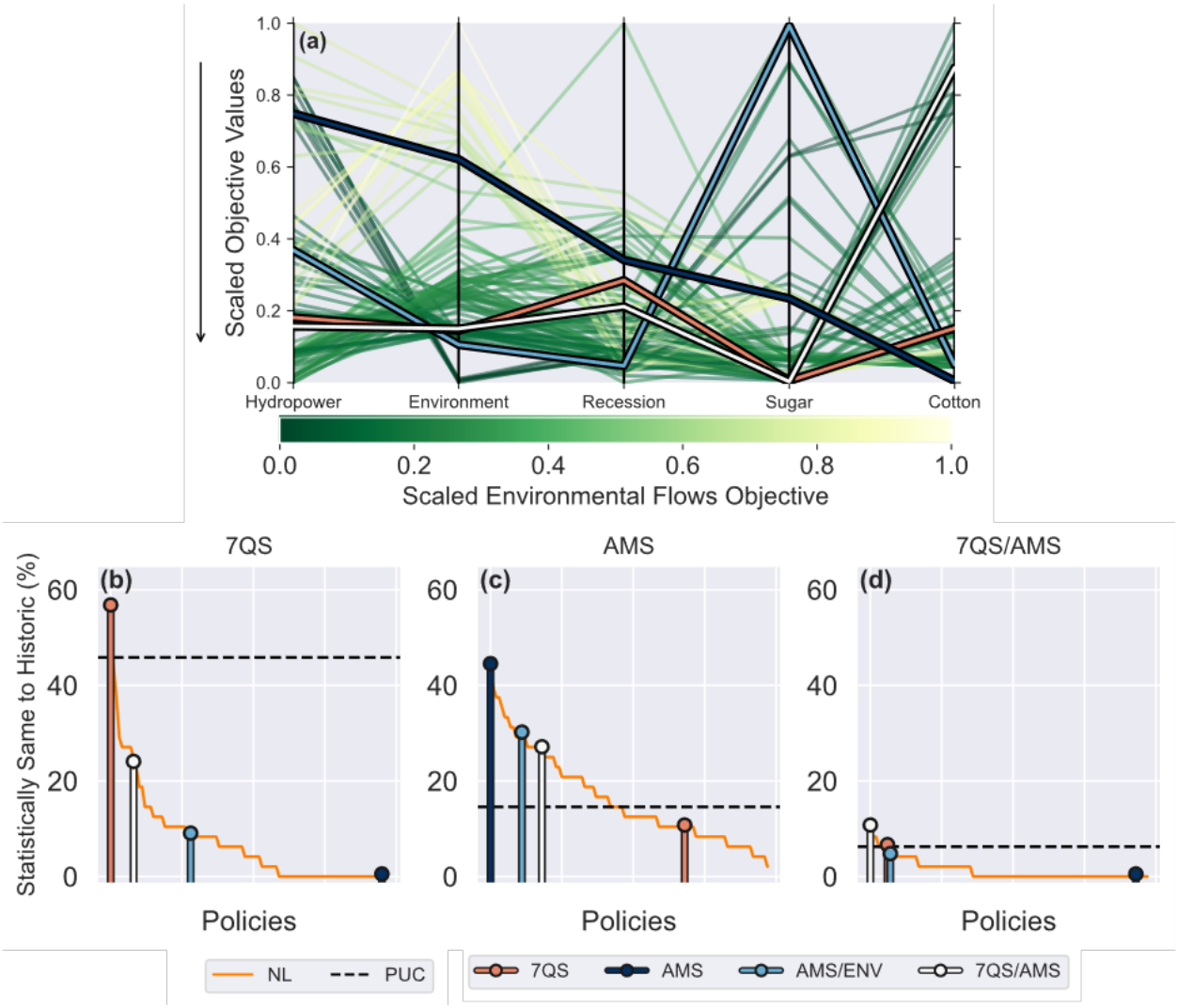

Figure 3.1: (a) Parallel axis plot showing historical tradeoffs of operating policies under historical conditions. Robust policies analyzed more deeply in this chapter are highlighted. (b) - (e) Performance on robustness metrics of all policies, sorted from highest to lowest on (b) 7QS, (c) AMS, and (d) both 7QS and AMS with policies that perform best on each metric highlighted. Policies with robustness metrics that are higher than the projected uncontrolled scenario (PUC) mitigate the impact of climate change while those with lower metrics exacerbate the impact of climate change. Results from late century are in Appendix Figure A.2

with the highest satisficing metric to the lowest. A black line also indicates the satisficing metric under projected uncontrolled conditions. In Figure 3.1b, we can see that only a few

policies perform better in preserving historical uncontrolled low flows than PUC, suggesting that the water infrastructure development typically dampens low flows. However, figure 3.1c shows that many policies preserve pre-dam high flow extremes better than the uncontrolled scenario. We will explore if this might be from reservoirs dampening increasingly high extreme flows, reservoirs supplementing decreased high flows in particularly dry projections, or a combination of the two. Finally, the most robust reservoir operating policy preserves pre-dam high *and* low flows in only about 11% of climate projections considered, highlighting the trade-off in mitigating these two different types of water resources extremes (Figure 3.1d). However, several policies maintain pre-dam extreme distributions of both AMS and 7QS in more projections than PUC.

From this analysis, we select several policies to analyze more deeply: the policies that best mimic pre-dam low flows (7QS), high flows (AMS), and both high and low flows (7QS/AMS) in the highest percentage of projections (Figure 3.1b-d). We find that the AMS policy significantly alters seasonality of flows downstream of the dams, so we also consider the next best policy for mimicking the distribution of pre-dam high flows that also performs better than PUC on the environmental flows objective across all climate projections (AMS/ENV). These four policies also perform best on their respective metrics at late century, except for the 7QS/AMS policy, which is replaced by the AMS/ENV policy as the best on both metrics (see Figure A.2).

Comparing these policies on the different robustness metrics, we see clear trade-offs between the policies: the best policy for AMS is the worst of the four policies in preserving historical low flows, and the best policy for 7QS is the worst of the four policies in preserving historical high flows. The AMS/ENV and the 7QS/AMS policies strike a better balance in managing these extremes, but still perform worse than PUC in preserving pre-dam low flows mid-century. However the 7QS/AMS and 7QS policies both outperform

PUC on the third satisficing metric, meeting both high and low flow satisficing conditions more often, and the 7QS/AMS outperforms PUC on all three metrics by late century (see Figure A.2).

Interestingly, while these policies have evident tradeoffs between high and low flow robustness, all but the AMS policy perform similarly (and quite well) on the environmental flows objective historically (Figure 3.1a). This highlights the importance of considering multiple ecological performance objectives, as policies that perform similarly on reproducing mean flows and seasonality targeted by the environmental flows objective may not be reproducing extremes in the same way. There is also equifinality in how these policies achieve similar environmental flows while favoring other objectives differently. The best policy for AMS/ENV is one of the best policies for environmental flows at the expense of sugarcane yields, whereas the best policy for AMS is one of the worst policies across all objectives except cotton yields, for which it is the optimal policy. This suggests that conditions favorable to cotton production incidentally reduce high flows. On the opposite extreme, the 7QS/AMS policy performs well across all objectives historically except cotton yields, while the 7QS policy achieves fairly strong performance across all objectives.

3.4.2 Trend Identification in Extremes for Select Policies

We next identify trends in high and low flows from historical observations to the end of mid-century for PUC and these four operating policies using the Mann-Kendall trend test to see if different operating policies can reduce their occurrence. We summarize the results in Figure 3.2, where we show the percent of projections with no trend from historical in gray, with an increasing trend in blue, and a decreasing trend in orange.

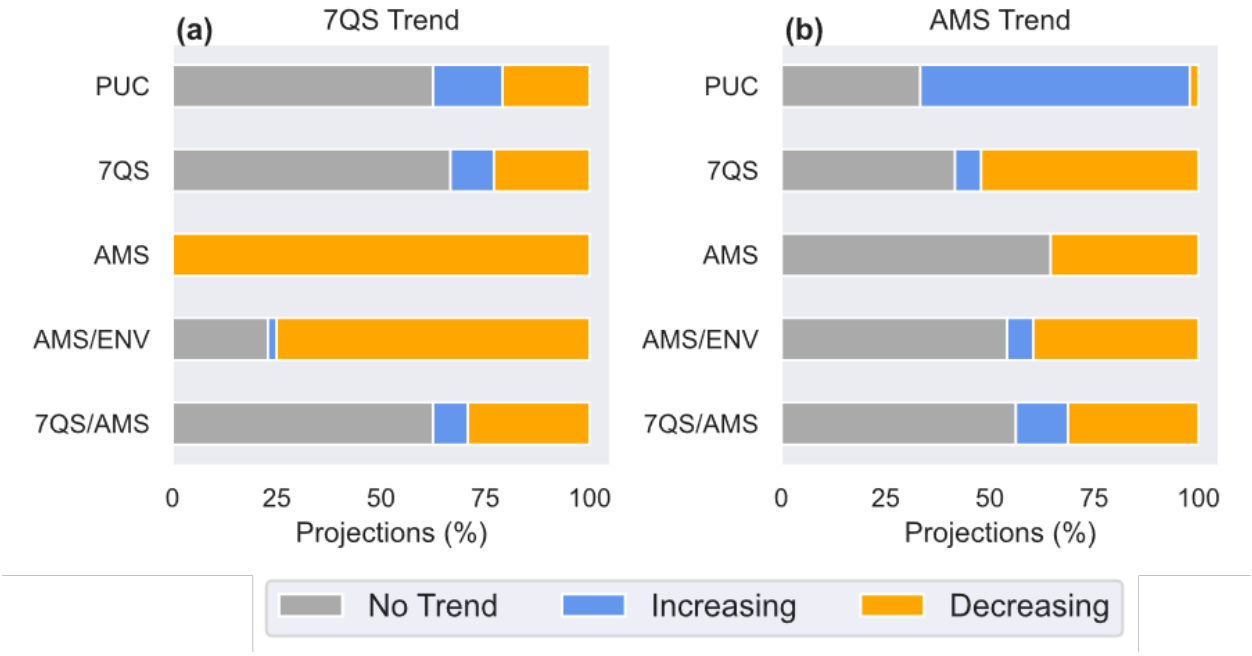

Figure 3.2: Breakdown of the percent of projections that show no trend, an increasing trend, or decreasing trend for PUC as well as 7QS, AMS, AMS/ENV, and 7QS/AMS policies for (a) seven-day low flows, and (b) annual maxima series. The late century results are in Appendix Figure A.3.

In absence of water infrastructure development, the seven-day low flows most commonly show no trend. The best policy for 7QS and 7QS/AMS share similar results to PUC (Figure 3.2a). However, we see that all of the AMS policies and most of the AMS/ENV policies show a decreasing trend in low flows, indicating unfavorable adaptation.

PUC most commonly has a statistically significant increasing trend on the annual maxima series in the Omo River from the historical time period to mid-century, which highlights the increased flood risk to downstream communities under climate change (Figure 3.2b). This could have negative implications for recession agriculture as well. The policies considered here clearly help mitigate that risk, increasing the share of projections under which there is no trend or a decreasing trend in the annual maxima series. Once again, 7QS/AMS proves to be a favorable compromise solution, yielding no meaningful change

in the number of projections with low flow trends while decreasing the number of projections with increasing high flow trends. By late century, these benefits are even stronger, as PUC exhibits more statistically significant low flow trends while 7QS/AMS does not (see Appendix Figure A.3).

3.4.3 Evaluation of Extremes Distributions for Select Policies

We visualize the distributions of high and low flows from the four operating policies and the projected uncontrolled conditions using a plot of their ECDFs at mid-century (Figure 3.3; see Appendix Figure A.4 for the end-of-century ECDFs). Each line represents a separate climate projection, colored by the average flow in the Omo Delta in that projection's uncontrolled scenario as a proxy for how wet or dry that climate projection is. The distribution under historical uncontrolled conditions (HUC) is shown in black. Projections where the time series of 7QS and AMS do not exhibit a statistically significant monotonic trend and where their distribution is statistically the same as HUC are shown in bold.

Projections produce a wider spread in extreme lows and extreme highs compared to HUC. This is unsurprising, as climate change is projected to cause both more severe droughts and more intense flooding (Trenberth, 2011; Boulange et al., 2021; Bates et al., 2008). PUC preserves historical low-flows fairly well, except for in the wettest and driest future conditions (plot a). However, uncontrolled scenarios only preserve the distribution of annual maxima in very dry projections, which suggests that there is an increased flood risk in most projections (plot b). The best policy for 7QS is able to preserve the distribution of low flows in many projections that are both wet and dry (plot c), but only preserves the distribution of AMS in a few moderately wet climate projections (plot d). While this suggests that this policy may dampen high flows in dry projections, its performance on the recession agriculture objective almost always outperforms PUC across

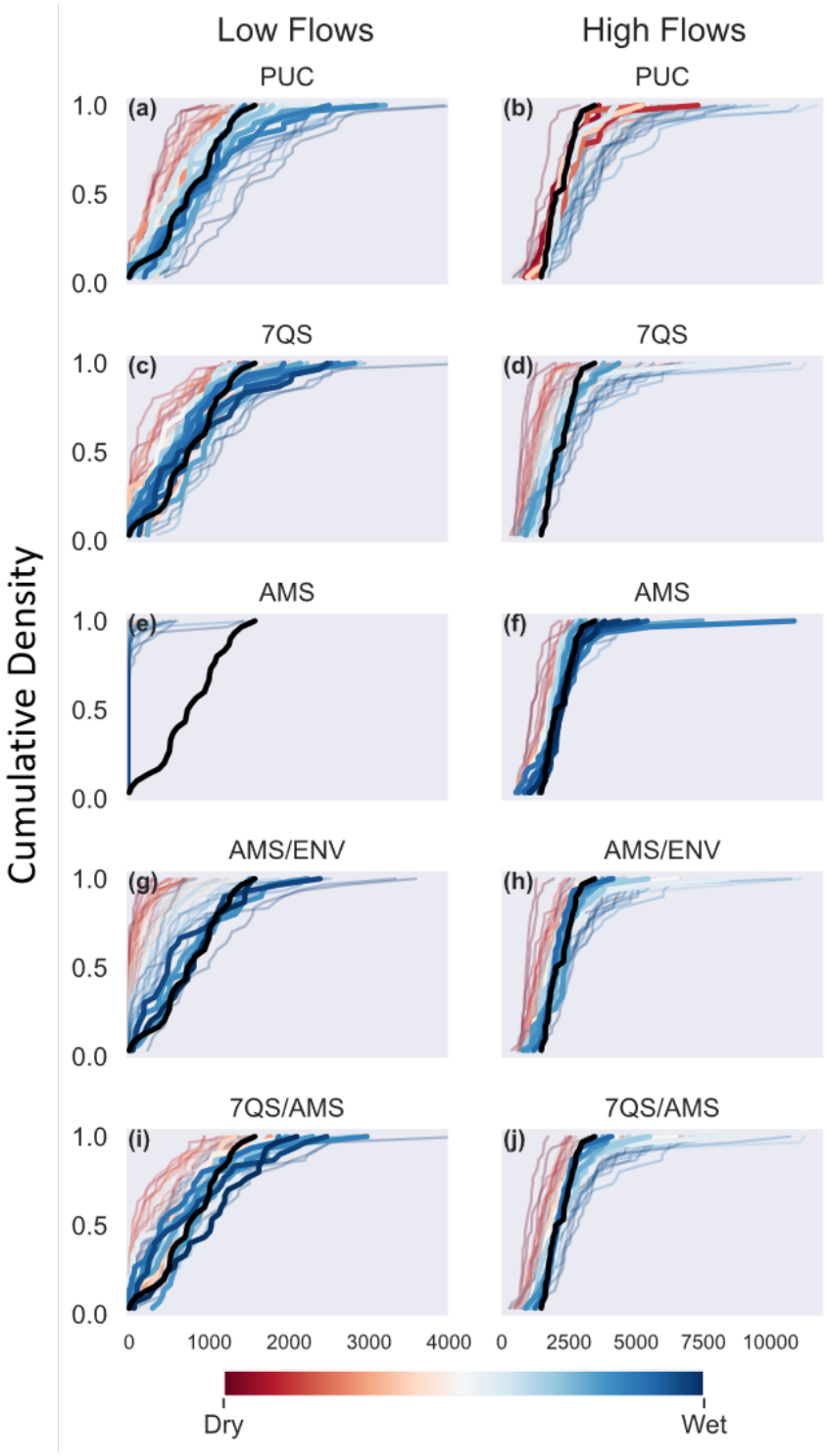

Figure 3.3: Empirical cumulative distributions of PUC, as well as 7QS, AMS, AMS/ENV, and 7QS/AMS policies seven-day low flows and annual maxima series. The ECDFs of HUC high and low flows are shown in black on each plot. Late century results are shown in Appendix Figure A.4.

projections (see Apendix Figure A.8). However, it fails to mitigate the most extreme flood events, where flows reach nearly 10,000 cms, which would be a devastating flood for indigenous populations in the Lower Omo Valley.

The best policy for AMS mirrors the HUC high flow distribution in many projections (plot f). However, this policy completely alters the distribution of low flows across all climate projections, severely reducing seven-day low flows (plot e). This would have a devastating effect on indigenous people and ecological health in the Lower Omo Valley. Future work should explore if reduced irrigation abstractions could improve socio-ecological outcomes from this policy without sacrificing a large portion of annual yields.

The 7QS/AMS and AMS/ENV policies both preserve the HUC distribution of high flows fairly well for moderately wet and dry projections but fail to replicate pre-dam conditions in very wet or dry projections (plot h,j). While the AMS/ENV policy does better than the AMS policy at preserving HUC seven-day low flows (plot g), it still only preserves the distribution in the wettest projections while dry and moderate projections have severely dampened low flows. The 7QS/AMS policy also has statistically smaller low flows in the driest projections, but does not dampen them as severely (plot i).

To understand how the high and low flow distributions are maintained better or worse with these different operating policies, we explore how their average daily reservoir storage levels change across the climate projections (Figure 3.4). Once again, the lines are colored by the average flow in the Omo Delta for that projection's uncontrolled scenario, with red lines representing the driest scenarios and blue lines representing the wettest scenarios.

Intuitively, for all these policies, wetter projections tend to yield higher reservoir levels and drier projections result in lower reservoir levels. However, the diverging management decisions result in some key differences in the actual magnitude of storage levels

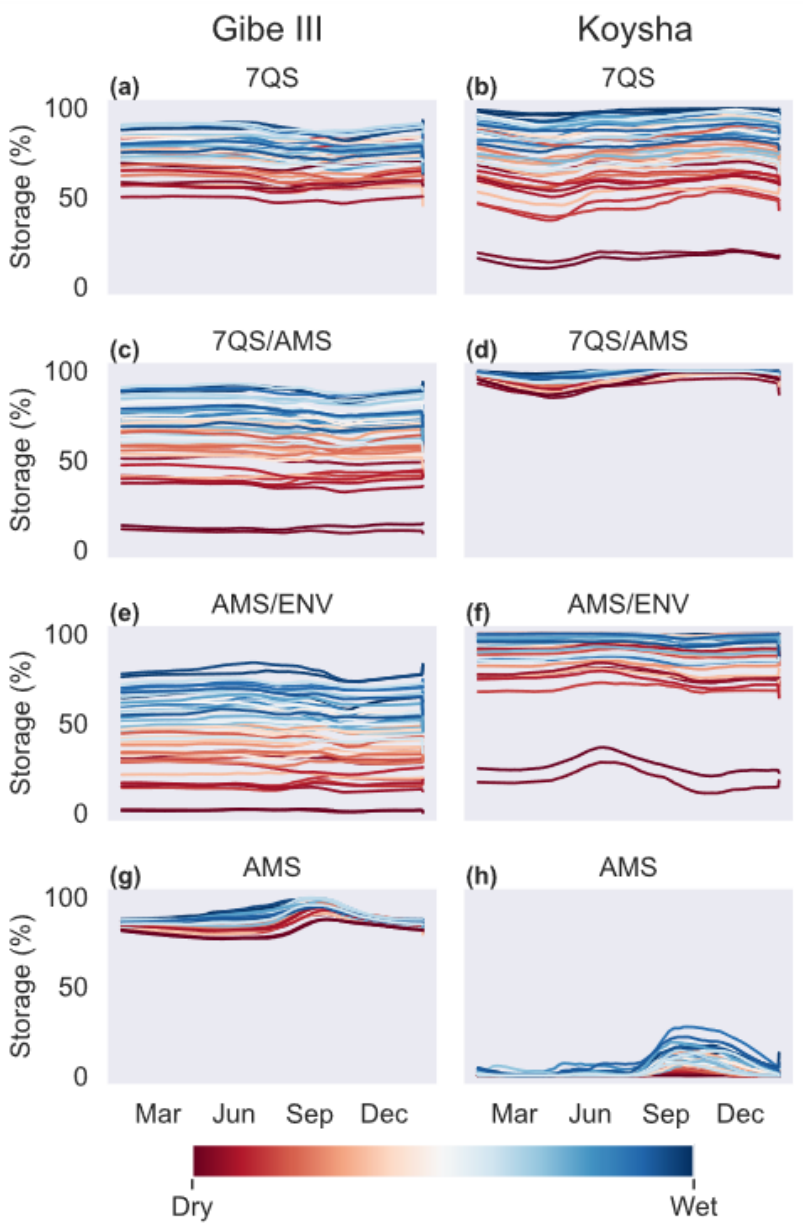

Figure 3.4: Average daily reservoir storage levels as a percent of operational capacity at Gibe III and Koysha for each of the robust policies. Each line represents storage levels in a single projection, with dry to wet projections colored from red to blue. Late century results are shown in Figure A.5.

across policies. The 7QS policy (plot a,b) tends to keep Gibe III levels fairly high – above 50% of the reservoir's operational storage capacity. Koysha has a wider range of reservoir storage levels, with the two driest projections dropping storage to just 25% of the reservoir's operational capacity on average. Maintaining fairly high reservoir levels while still allowing storage to drop in dry conditions likely creates water availability during the dry season. It also enables high hydropower production (Figure 3.1). However, the ability to maintain relatively high levels is likely a result of storing inflows during the wet season, which could dampen annual high flows, particularly during dry years.

The 7QS/AMS and AMS/ENV policies both have a wider spread of average storage levels at Gibe III and a much tighter range of average daily levels at Koysha compared to the 7QS policy. Dropping levels at Gibe III more in dry conditions allows levels at Koysha to stay high, and provides more consistent water downstream to mirror historic annual mean, high, and low flows.

Finally, reservoir levels for the AMS policy indicate how unanticipated behavior can arise from multi-objective reservoir operations. Levels are kept extremely high at Gibe III and low at Koysha, with very little variability between wet and dry projections. There is clearly adequate supply in Gibe III to release to Koysha during the dry season and produce flows that would produce better ecological outcomes, but this policy favors cotton yields over all other objectives. During the wet season, Koysha fills slightly in the wettest projections, reducing downstream flows and therefore annual maxima that would otherwise increase unfavorably. This is an unintended side effect of the policy altering the downstream seasonality to be more favorable for cotton production.

3.4.4 Evaluation of Flow Distributions Throughout the Year for Select Policies

For each policy, we use simulated flows in the Omo River delta across projections to estimate the relative frequency of observing different flow magnitudes downstream of the dams over the course of the year. Figure 3.5 shows the percent of simulated years in which the flow was at different magnitudes each calendar day, with high frequencies shaded red, moderate frequencies yellow, and low frequencies blue. The solid black lines show the historical daily high and low flow magnitudes for each day of the year and the dashed black line shows the historical daily median. While certain projections produced flows higher than 4,000 cms, we bound the plot to this range for visualization purposes because (a) flow events greater than 4,000 cms are so rare that they are difficult to see on the plot and (b) we already explored how the distribution of extremes changed in section 3.4.3.

The shape of the frequency distributions is similar over time, with flows of the highest frequency in red rising in July for the rainy season and decreasing again in late October, generally mirroring the historical median. However, there are some key differences between these policies. While the AMS policy reduces the likelihood of flows above the historical maximum compared to the projected uncontrolled scenarios, it completely alters the seasonality of flows in the Omo River, with the wet season peak flows arriving later than their historical peak (plot b). Furthermore, as we observed before, the AMS policy frequently dewaters the Omo River downstream of the dam, as shown by the high frequency of observing 0 cms from January to June. The AMS/ENV policy's flows almost always lie within historical bounds (plot c). This policy far outperforms the others in avoiding dampened flows during the wet season from July to October, since barely any simulations fall in this region. This policy also satisfies an additional robustness metric, as this was the best policy for preserving the historical distribution of the AMS that also

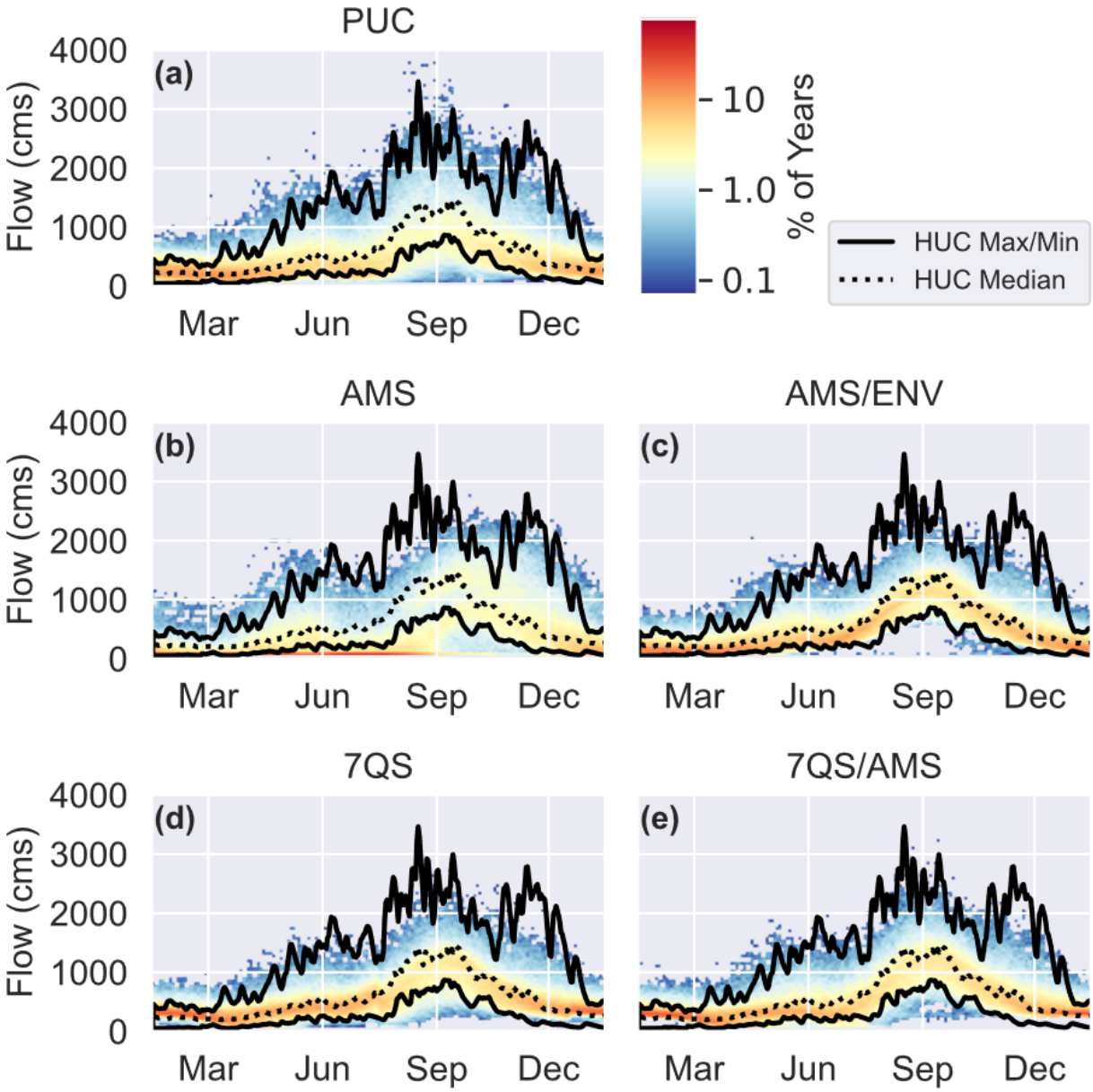

Figure 3.5: The percent of simulated years where the flow was at different magnitudes on each calendar day, with high frequencies in red and low frequencies in blue for (a) PUC, (b) AMS (c) AMS/ENV, (d) 7QS, (e) 7QS/AMS. Maximum and minimum daily HUC flows are shown with the black solid line and the median daily HUC flows are represented by a dotted black line. Late century results are in Appendix Figure A.7.

performed better than the uncontrolled scenario on our environmental flows objective across all projections (see Appendix Figure A.8). This plot highlights the power of that policy design in preserving historical flows, particularly during the wet season. The most frequent flows of the best 7QS policy during the dry period from January to March are notably higher than for all other policies, falling at or slightly above the historical median (plot d). The 7QS/AMS policy's flows have similar frequencies to the 7QS policy throughout the year (plot e).

These plots demonstrate that, with the exception of the best AMS policy, the reservoir operating strategies that mitigate extremes help draw flows towards their historical pattern, particularly compared to future projected scenarios that do not involve any infrastructure development. The AMS/ENV, 7QS, and 7QS/AMS policies all reduce the likelihood of flows falling outside of their historical maximum and minimum values across all days of the year under climate change conditions. These near-natural flow conditions also enable continued recession agriculture downstream. Furthermore, they are achieved despite also drawing irrigation water for sugar and cotton production, and while producing a clean source of power. Policy performance for these policies on all objectives across all projections is shown in Appendix Figure A.8. This illustrates how well-designed multi-objective reservoir operations can facilitate win-win climate adaptation.

3.5 CONCLUSIONS

This study evaluates the robustness of closed-loop, nonlinear reservoir operating policies in mitigating the impact of climate change on floods and droughts in the Omo River basin. We find that it is difficult to design policies that can mitigate both flood and drought extremes under climate change, as we observe tradeoffs in the performance of policies that best mitigate high flows vs. low flows. Furthermore, while many policies replicate his-

torical mean flows, they do not necessarily reproduce extremes in the same way. This underlines the importance of exploring policy performance beyond historically defined objectives when considering climate change, as policies that perform similarly on our environmental flows objective have significantly different outcomes for high and low flow extreme events across climate change projections.

However, we also demonstrate that water infrastructure development can improve climate resilience, since compromise reservoir operating policies can produce more balanced socio-ecological outcomes while mitigating extremes. This highlights the value of multi-objective optimization in producing a set of alternative operations to choose from, and in performing climate stress tests to inform that selection. Here, we were able to find a compromise solution that mitigated the impacts of changing high and lows flows compared to a projected uncontrolled scenario at the end of the century while also improving other system objectives. However, many policies actually had worse robustness metrics than the projected uncontrolled scenario, and simpler design procedures may have only discovered these policies. Future work incorporating forecasts into the policy design could further improve performance in the compromise region, as season-ahead forecasts could be used to adapt reservoir storage levels up or down in a way that mitigates increasing high flows or decreasing low flows while maintaining favorable socio-ecological outcomes.

CHAPTER 4

Conclusions and Future Work

In this study, we first advance the representation of reservoir operations in SWAT to simulate state-aware, nonlinear operating policies. We demonstrate that the updated reservoir module can better balance multisectoral water demands than the model's original reservoir operations in a case study in the Omo River basin. We then leverage these model advancements to demonstrate that optimized nonlinear reservoir operating policies can be used to mitigate the impact of climate change on extreme flow events while still balancing economic, agricultural, social, and ecological outcomes.

This work highlights the potential for using the updated reservoir module in SWAT to understand which policies are robust to different exogenous changes in the Omo River basin, such as climate, continued dam construction, increased development of irrigable agriculture, altered infrastructure efficiency, alternative irrigation and fertilizer applications, and more. In this study, we consider robustness to climate change, but SWAT is a useful tool for quantifying the effects of the human decisions and actions mentioned above in tandem with changing system conditions (Abbaspour et al., 2015; Wang et al., 2016). Integration of this model with ABMs or other decision support tools that enable two-way feedbacks between human decisions and environmental outcomes would open the door to deeper robustness analyses of reservoir operating policies.

A completely revised and reconstructed version of SWAT, named SWAT+ was recently released, which includes an updated reservoir module (Wu et al., 2020). Reservoir releases are still defined by storage-outflow relationships, but the module includes additional parameters to define release rules that allow for more nuanced and flexible operations. It would be interesting perform an additional study comparing the performance of our nonlinear operating policies to the updated storage-outflow reservoir module in

SWAT+.

Finally, it is important to highlight that, while we demonstrate that reservoirs can help mitigate the impact of climate change and improve multisectoral outcomes in the Omo River basin, we also create a model where Koysha has been fully built and filled, and the agricultural lands for sugarcane and cotton have already been developed. In reality, as of October 2020, Koysha was less than 50% complete (Geeska Afrika Online, 2020) and agricultural developments are still in progress (Human Rights Watch, 2017). The filling phase of the Gibe III dam eliminated the annual flood pulse in the Lower Omo Valley and Lake Turkana dropped 1.7 meters, which had a dramatic impact on riverine ecosystems and indigenous agropastoralists (Avery, 2017; Human Rights Watch, 2017; Avery & Tebbs, 2018; IUCN, 2018). Zaniolo et al. (2021) show that properly timing the filling phase with climate oscillations with adaptive filling operations could have reduced socio-ecological costs associated with filling Gibe III; however, they anticipate similar negative socio-ecological outcomes as Koysha fills unless such strategies are employed. Furthermore, since we assume that irrigated agricultural development will proceed as planned, we do not balance the social and economic outcomes of arriving at this state. In reality, the social impacts of these agricultural developments are steep: human rights violations, including forced evictions, beatings, and other abuses of indigenous people, are well documented as the Kuraz Sugar Development Project advances (Oakland Institute, 2019). Since we have demonstrated that reservoirs in the Omo River can balance socio-ecological tradeoffs when the development is already operational, future work should focus on how we can get to that point ethically and sustainably.

APPENDIX A

Appendix

A.1 TABLES

Table A.1: Maximum and minimum boundaries of the parameters and fitted values after calibration. Parameters followed by _f are relative changes.

Parameter Name	Lower Bound	Upper Bound	Calibrated Value
CN2_f	0.70	1.25	0.78
ESCO	0.01	1	0.39
EPCO	0.01	1	0.97
ALPHA_BF	0.001	1	0.005
GWQMN	0	6000	3900
GW_REVAP	0.02	0.2	0.19
REVAPMN	0	1000	513
SURLAG	0.1	12	0.32
AWC_f	0.85	1.25	1.01
DEPTH_f	0.85	1.25	1.18
KSAT_f	0.85	1.25	0.85
BD_f	0.80	1.15	0.81
SLSOIL_f	0.75	1.25	1.00
OV_N_f	0.85	1.25	0.995

Table A.4: RC Objective Values

	Performance on:				
Best Policy For:	***Hydropower***	***Environment***	***Recession***	***Sugar***	***Cotton***
Hydropower	-549	0.104	9.716	-3359262907	-23641721
Environment	-520	0.046	0.211	-3278217408	-24247490
Recession	-530	0.100	**0.001**	-3423907768	-26821469
Sugar	-538	0.143	0.493	**-3435442807**	-24227202
Cotton	-531	0.130	0.099	-3338718564	**-27131235**

Table A.2: CMIP5 climate projections used in the study

Model	RCP			
	2.6	***4.5***	***6.0***	***8.5***
ACCESS 1.0	-	✓	-	✓
CCSM4	-	✓	✓	✓
CESM1-BGC	-	✓	-	✓
CMCC-CESM	-	-	-	✓
CMCC-CMS	-	✓	-	✓
CMCC-CM5	✓	✓	-	-
CSIRO-Mk3.6.0	✓	✓	✓	✓
GFDL-CM3	✓	-	✓	✓
GFDL-ESM2G	✓	✓	✓	✓
GFDL-ESM2M	✓	✓	✓	✓
HadGEM2-CC	-	✓	-	✓
HadGEM2-ES	-	-	✓	-
MIROC-ESM-CHEM	✓	✓	✓	✓
MIROC-ESM	✓	✓	✓	✓
MPI-ESM-LR	✓	✓	-	✓
MPI-ESM-MR	✓	✓	-	✓
NorESM-M	✓	✓	✓	✓

Table A.3: Epsilon values during optimization and for thinning Pareto approximation sets.

	Hydropower	**Environment**	**Recession**	**Sugar**	**Cotton**
Optimization	2.0	0.01	0.3	1260000.0	41000.0
Thinning	8.0	0.03	1.0	3800000.0	150000.0

Table A.5: NL Objective Values

Best Policy For:	Performance on: *Hydropower*	*Environment*	*Recession*	*Sugar*	*Cotton*
Hydropower	**-559**	0.141	14.076	-3404849164	-26545307
Environment	-455	**0.026**	0.895	-3176994259	-24320836
Recession	-465	0.060	**0.002**	-3181897845	-26898950
Sugar	-486	0.041	1.476	**-3435155667**	-24088818
Cotton	-465	0.274	1.622	-3332858938	**-27124587**

A.2 FIGURES

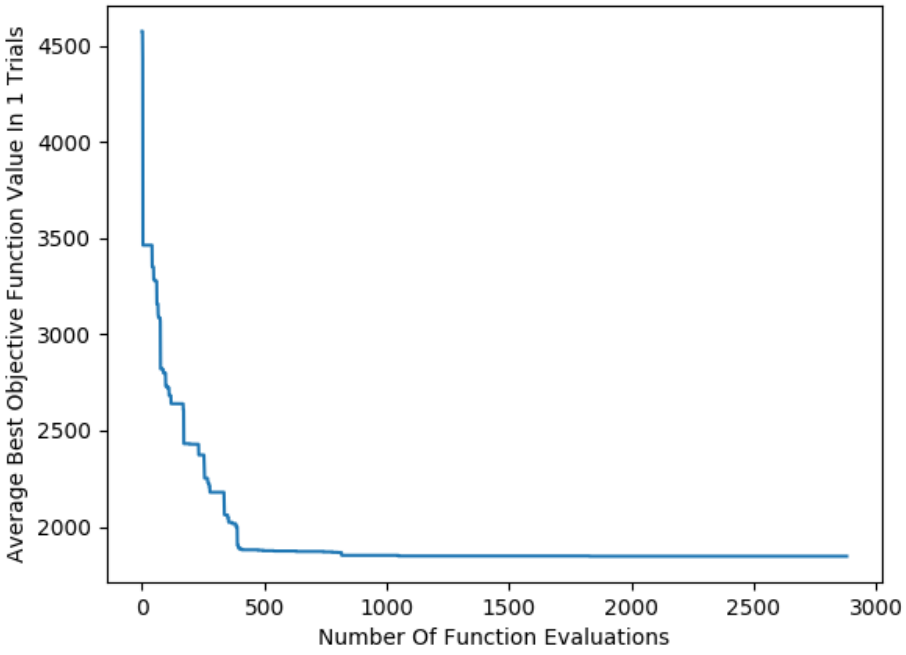

Figure A.1: Objective function value for each number of function of evaluations (NFE) over the course of 24-hour DDS SWAT calibration of the best calibration trial. The objective value converges, indicating adequate calibration runtime.

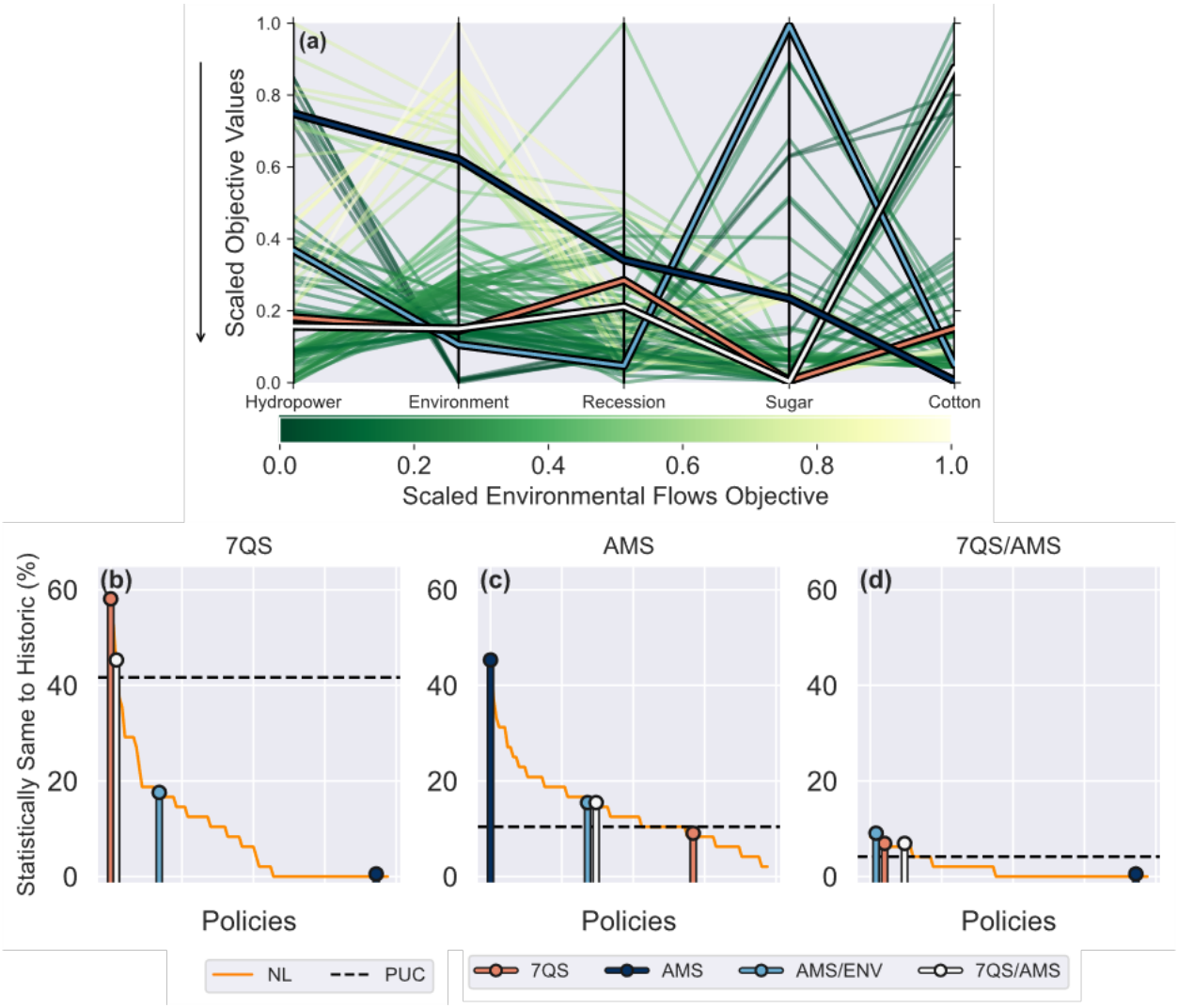

Figure A.2: (a) Parallel axis plot showing historical tradeoffs of operating policies under historical conditions. Robust policies analyzed more deeply Chapter 3 are highlighted. (b) - (e) Performance on robustness metrics of all policies, sorted from highest to lowest on (b) 7QS, (b) AMS, and (c) both 7QS and AMS. Policies that perform best on each metric at mid-century are highlighted. Policies with robustness metrics that are higher than the projected uncontrolled scenario mitigate the impact of climate change while those with lower metrics exacerbate the impact of climate change. Results from mid-century are in Figure 3.1. The best policies for 7QS and AMS at mid-century are still the best at late century, while the AMS/ENV policy becomes the best policy for maintaining both 7QS and AMS. More policies beat PUC on our robustness metrics at late century than mid-century.

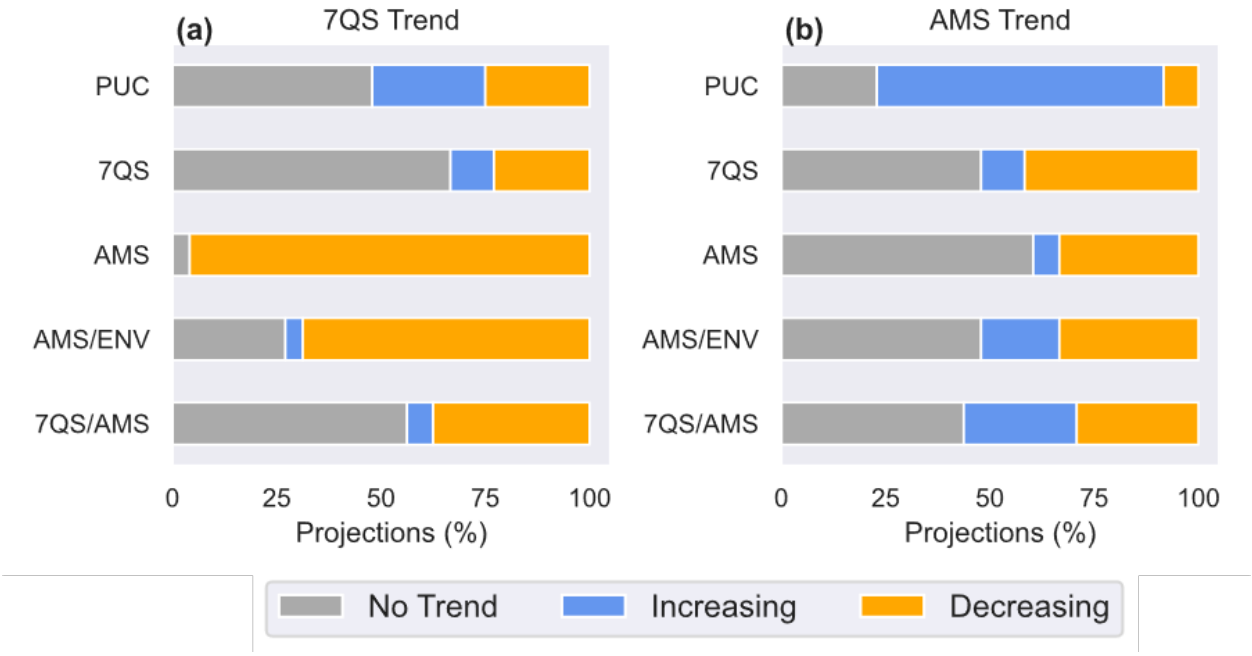

Figure A.3: Breakdown of the percent of projections that show no trend, an increasing trend, or decreasing trend for PUC as well as 7QS, AMS, AMS/ENV, and 7QS/AMS policies for (a) seven-day low flows, and (b) annual maxima series. The mid-century results are in Figure 3.2.

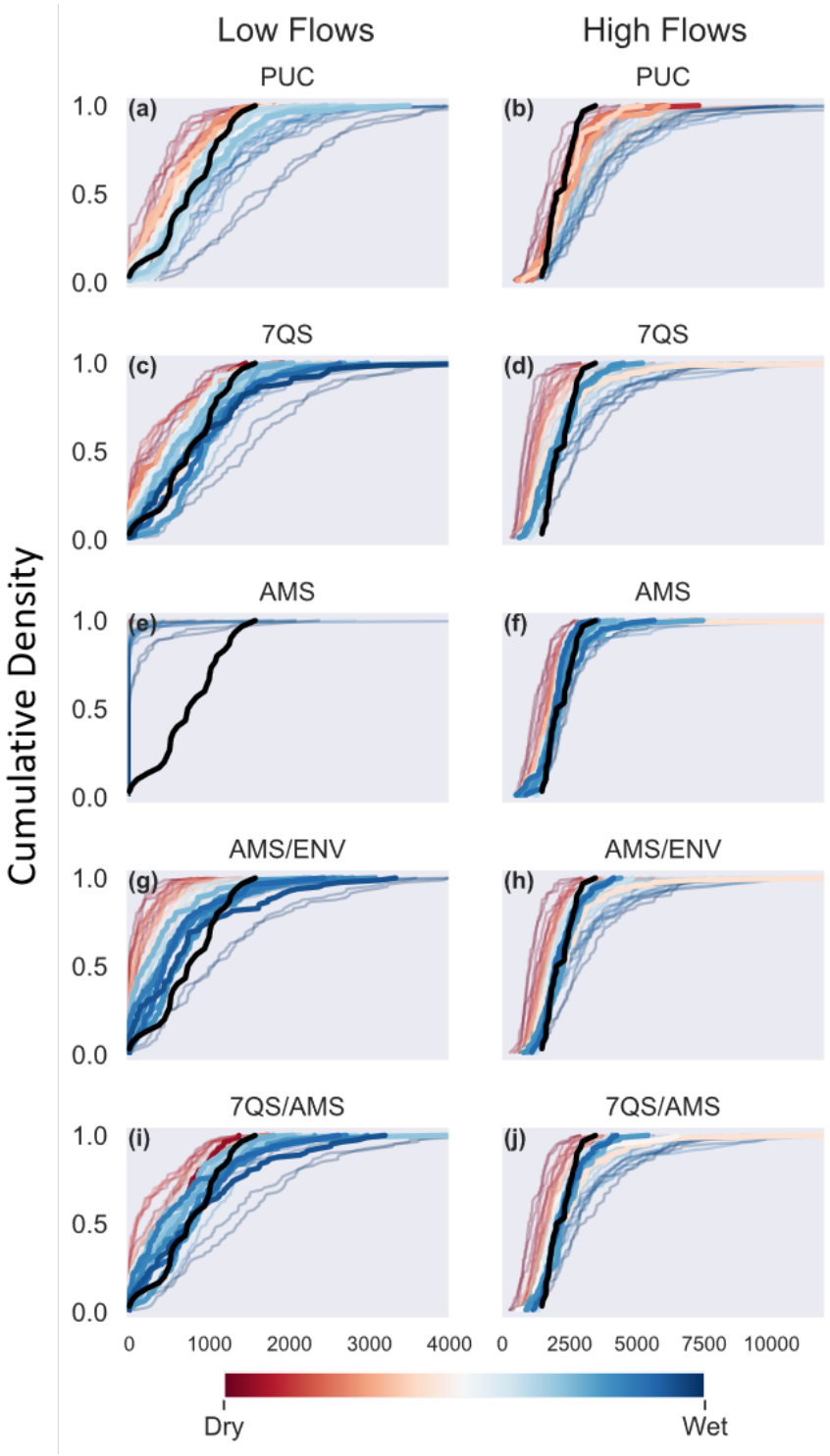

Figure A.4: Empirical cumulative distributions of PUC, as well as 7QS, AMS, AMS/ENV, and 7QS/AMS policies seven-day low flows and annual maxima series. The ECDFs of HUC high and low flows are shown in black on each plot. The results from mid-century are in Figure 3.3. ECDFs of wet projections are particularly different from HUC.

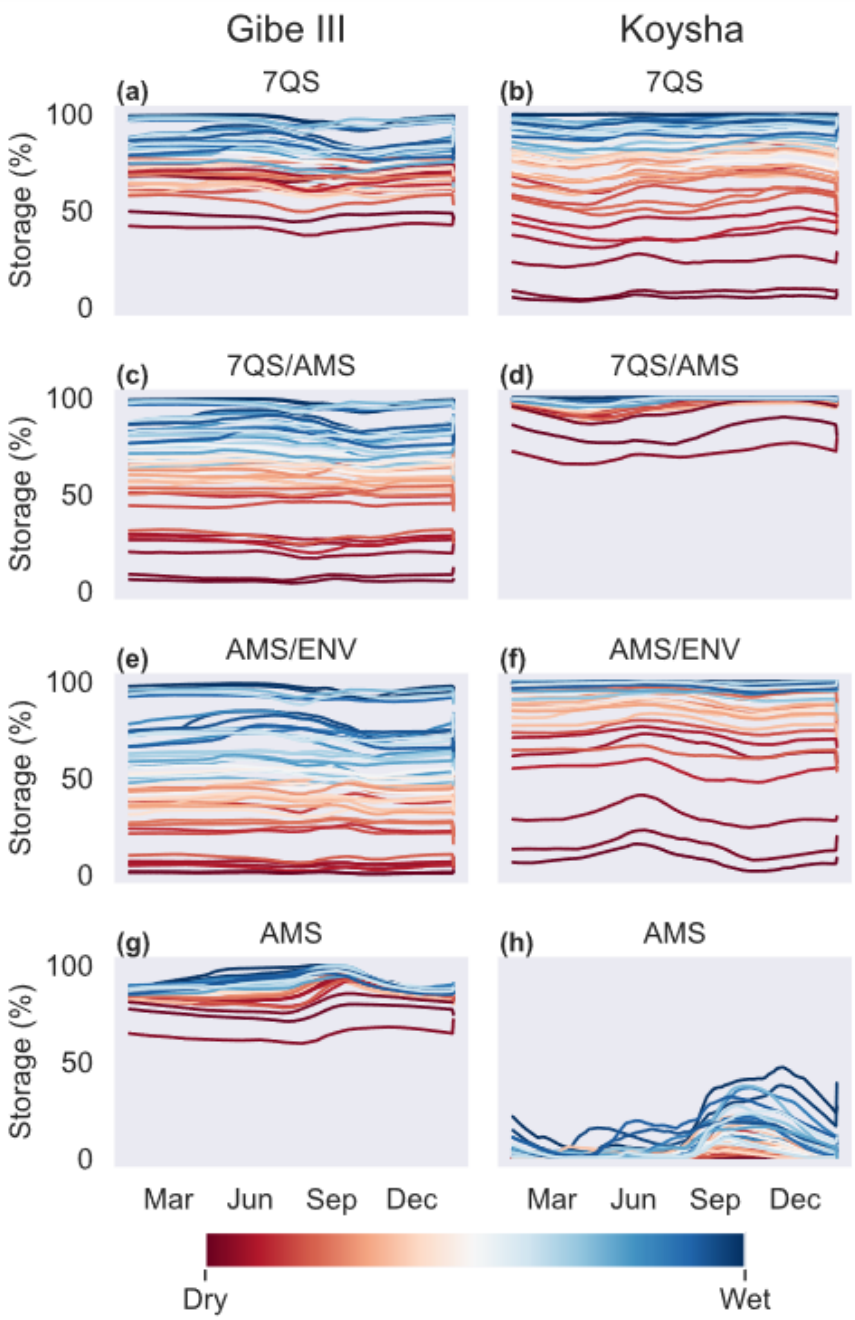

Figure A.5: Average daily reservoir storage levels as a percent of operational capacity at Gibe III and Koysha for each of the robust policies. Each line represents storage levels in a single projection, with dry to wet projections colored from red to blue. Mid-century results are shown in Figure 3.4. Average daily reservoir levels are more spread out between projections at late century than they were at mid-century, since wet and dry extremes become more pronounced.

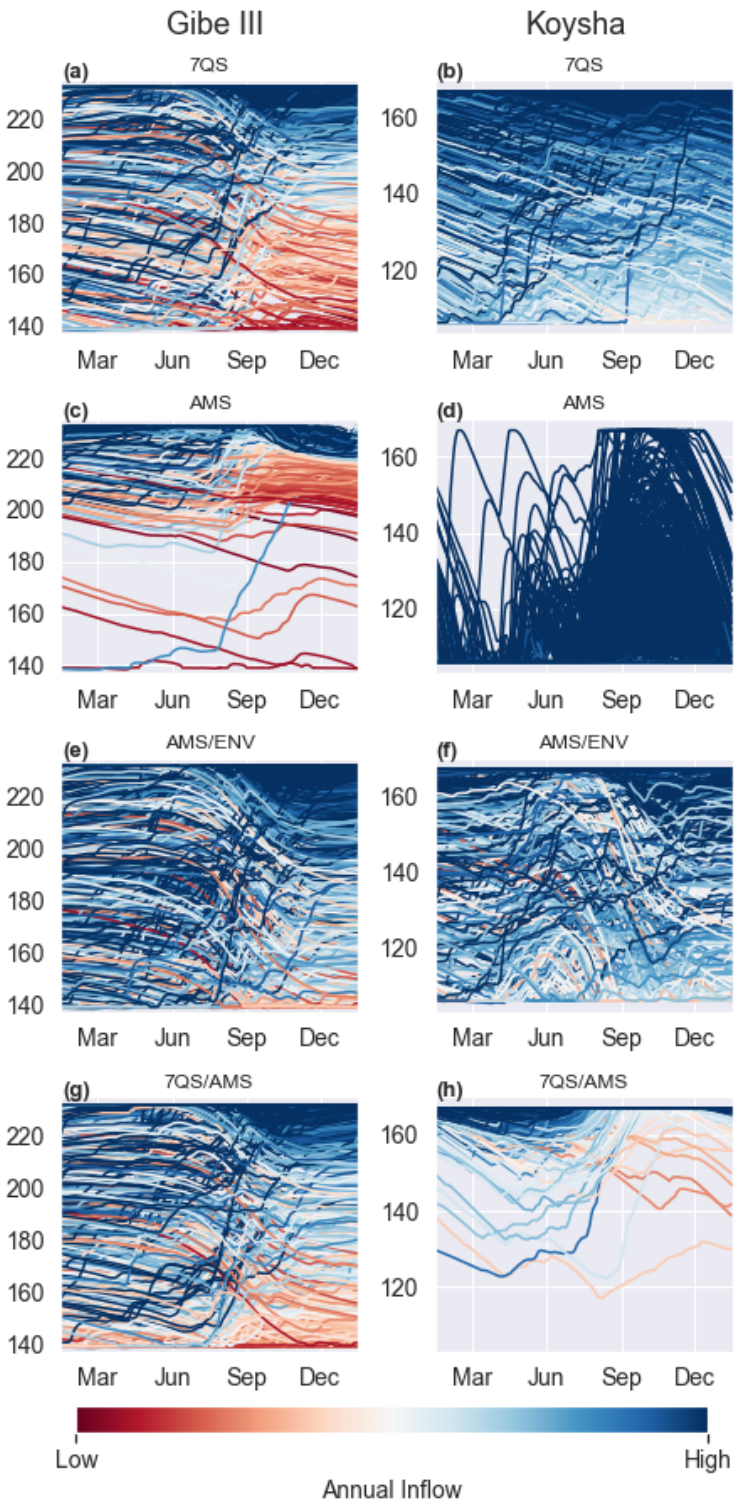

Figure A.6: Daily reservoir levels from each year of each projection at Gibe III and Koysha. Each line is colored by the annual inflow for a given projection and a given year, with the driest years in red and the wettest years in blue. We can see how reservoir levels drop in dry years and rise in wet years.

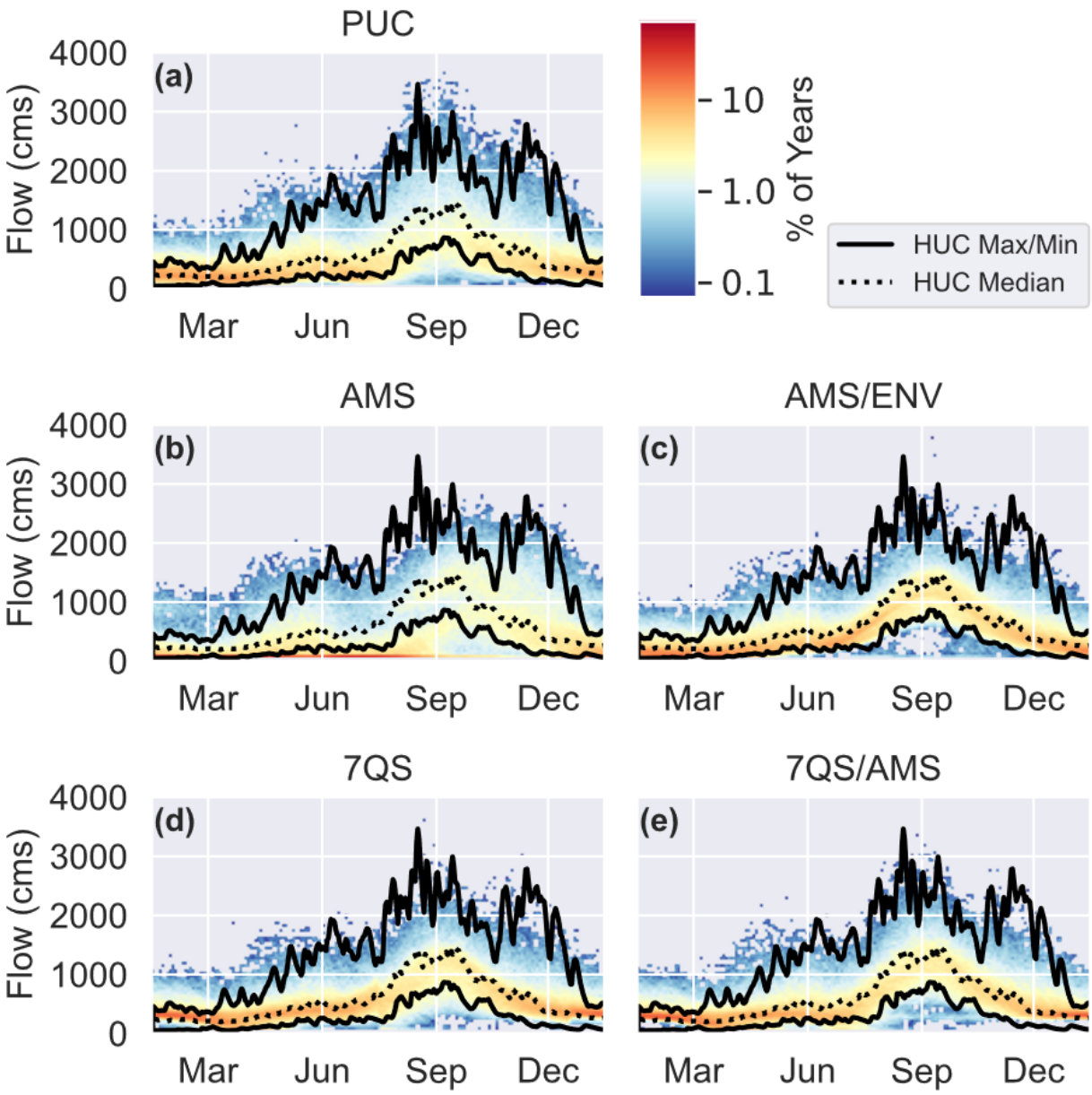

Figure A.7: The percent of simulated years where the flow was at different magnitudes on each calendar day, with high frequencies in red and low frequencies in blue for (a) PUC, (b) AMS (c) AMS/ENV, (d) 7QS, (e) 7QS/AMS. Maximum and minimum daily HUC flows are shown with the black solid line and the median daily HUC flows are represented by a dotted black line. Mid-century results are in Appendix Figure 3.5.

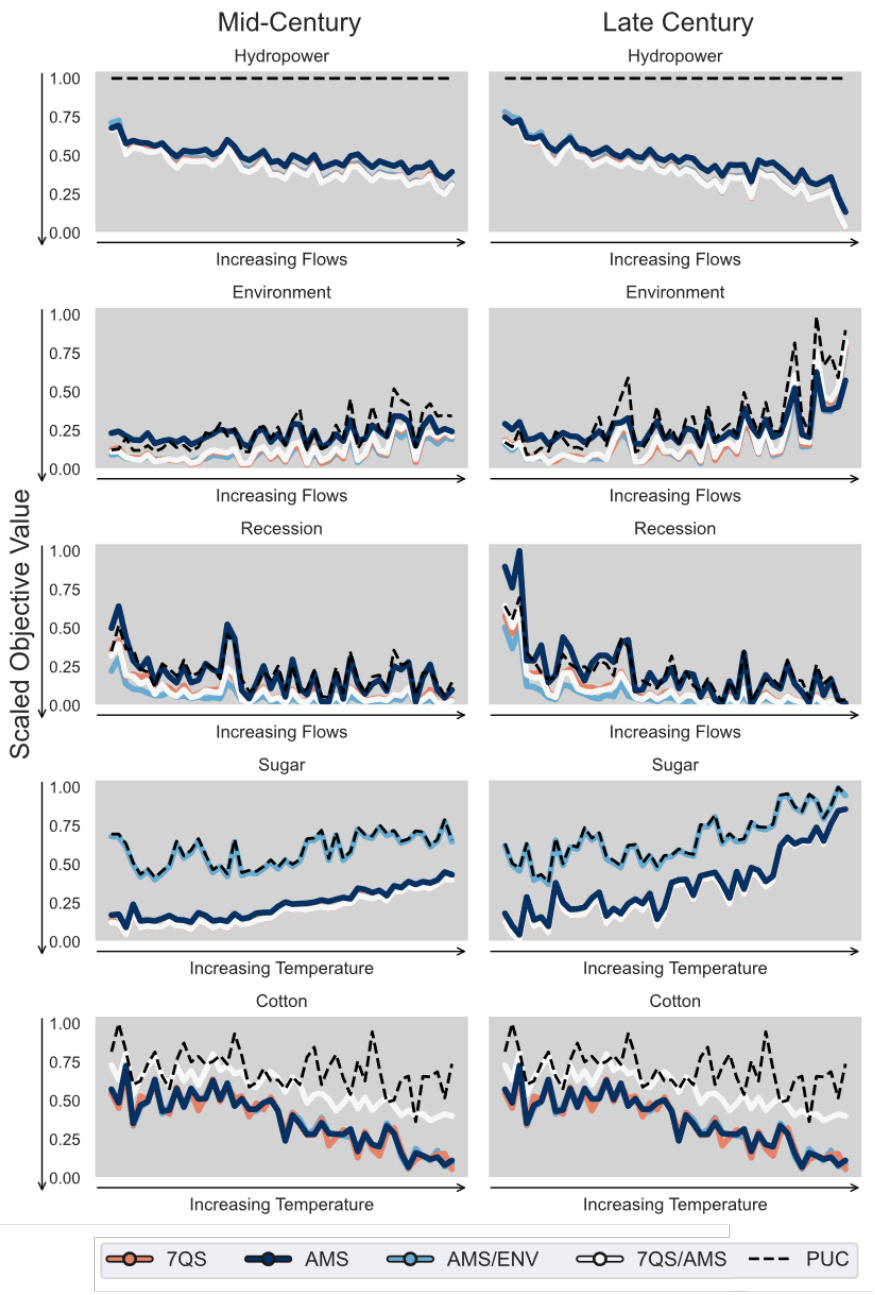

Figure A.8: Performance of robust policies on each objective under climate change at mid- and late century. These policies tend to perform as well or better than uncontrolled across most objectives and projections.

BIBLIOGRAPHY

Abbaspour, K. C., Rouholahnejad, E., Vaghefi, S., Srinivasan, R., Yang, H., & Kløve, B. (2015). A continental-scale hydrology and water quality model for europe: Calibration and uncertainty of a high-resolution large-scale swat model. *Journal of hydrology*, *524*, 733–752.

Abbink, J. (2012). Dam controversies: contested governance and developmental discourse on the ethiopian omo river dam. *Social anthropology*, *20*(2), 125–144.

Arnold, J. G., D. N. Moriasi, P. W. Gassman, K. C. Abbaspour, M. J. White, R. Srinivasan, C. Santhi, R. D. Harmel, A. van Griensven, M. W. Van Liew, N. Kannan, & M. K. Jha (2012). SWAT: Model Use, Calibration, and Validation. *Transactions of the ASABE*, *55*(4), 1491–1508.

Arnold, J. G., Srinivasan, R., Muttiah, R. S., & Williams, J. R. (1998). Large Area Hydrologic Modeling and Assessment Part I: Model Development1. *JAWRA Journal of the American Water Resources Association*, *34*(1), 73–89. _eprint: https://onlinelibrary.wiley.com/doi/pdf/10.1111/j.1752-1688.1998.tb05961.x.

Asress, M. B., Simonovic, A., Komarov, D., & Stupar, S. (2013). Wind energy resource development in ethiopia as an alternative energy future beyond the dominant hydropower. *Renewable and Sustainable Energy Reviews*, *23*, 366–378.

Avery, S. (2010). Hydrological impacts of ethiopia's omo basin on kenyas lake turkana water levels & fisheries.

Avery, S. (2012). Lake turkana & the lower omo: hydrological impacts of major dam and irrigation developments. *African Studies Centre, the University of Oxford*.

Avery, S. (2014). What future for lake turkana and its wildlife. *SWARA, Jan–Mar*.

Avery, S. (2017). Fears over ethiopian dams costly impact on environment, people. https://theconversation.com/fears-over-ethiopian-dams-costly-impact-on-environment-people-80757.

Avery, S. T., & Tebbs, E. J. (2018). Lake turkana, major omo river developments, associated hydrological cycle change and consequent lake physical and ecological change. *Journal of Great Lakes Research*, *44*(6), 1164–1182.

Babbitt, B. (2002). What Goes Up, May Come Down: Learning from our experiences with dam construction in the past can guide and improve dam removal in the future. *BioScience*, *52*(8), 656–658. Publisher: [American Institute of Biological Sciences, Oxford University Press].

Badagliacca, R., & Spinelli, L. (2018). Designing robust and sustainable development pathways in the omo-turkana basin, master's thesis.

Bates, B., Kundzewicz, Z., & Wu, S. (2008). *Climate change and water*. Intergovernmental Panel on Climate Change Secretariat.

Boulange, J., Hanasaki, N., Yamazaki, D., & Pokhrel, Y. (2021). Role of dams in reducing global flood exposure under climate change. *Nature Communications*, *12*(1), 417. Bandiera_abtest: a Cc_license_type: cc_by Cg_type: Nature Research Journals Number: 1 Primary_atype: Research Publisher: Nature Publishing Group Subject_term: Climate-change impacts;Hydrology Subject_term_id: climate-change-impacts;hydrology.

Carr, C. J. (2017a). Components of Catastrophe: Social and Environmental Consequences of Omo River Basin Development. In C. J. Carr (Ed.) *River Basin Development and Human Rights in Eastern Africa A Policy Crossroads*, (pp. 75–84). Cham: Springer International Publishing. https://doi.org/10.1007/978-3-319-50469-8_5 (Accessed:2021-06-19).

Carr, C. J. (2017b). The rush to rationalize: Public policies and impact assessments. In *River Basin Development and Human Rights in Eastern AfricaA Policy Crossroads*, (pp. 85–110). Springer.

Cole, M. A., Elliott, R. J. R., & Strobl, E. (2014). Climate Change, Hydro-Dependency, and the African Dam Boom. *World Development*, *60*, 84–98.

Copernicus Climate Change Service (2019). C3s era5-land reanalysis.

Davidson, W. (2015). Ethiopia may ship sugar in 2016 as india-backed plant read.

Dowd, C. (2020). A new ecdf two-sample test statistic. *arXiv preprint arXiv:2007.01360*.

EEPCO (2008). Environmental and social impact assessment executive summary, gibe iii hydroelectric power project.

EEPCO (2009). Gibe iii hydroelectric project environmental and social impact assessment additional study on downstream impact.

Ehsani, N., Vörösmarty, C. J., Fekete, B. M., & Stakhiv, E. Z. (2017). Reservoir operations under climate change: Storage capacity options to mitigate risk. *Journal of Hydrology*, *555*, 435–446.

ESA (2017). Land cover cci product user guide version 2.

Fratkin, E. (2014). Ethiopia's pastoralist policies: development, displacement and resettlement. *Nomadic Peoples*, *18*(1), 94–114.

Funk, C., Peterson, P., Landsfeld, M., Pedreros, D., Verdin, J., Shukla, S., Husak, G., Rowland, J., Harrison, L., Hoell, A., & Michaelsen, J. (2015). The climate hazards infrared precipitation with stationsa new environmental record for monitoring extremes. *Scientific Data*, *2*(1), 150066. Bandiera_abtest: a Cg_type: Nature Research Journals Number: 1 Primary_atype: Research Publisher: Nature Publishing Group Subject_term: Atmospheric dynamics;Attribution;Climate-change impacts;Environmental sciences;Hydrology Subject_term_id: atmospheric-dynamics;attribution;climate-change-impacts;environmental-sciences;hydrology.

Gassman, P. W., Sadeghi, A. M., & Srinivasan, R. (2014). Applications of the SWAT Model Special Section: Overview and Insights. *Journal of Environmental Quality*, *43*(1), 1–8. _eprint: https://acsess.onlinelibrary.wiley.com/doi/pdf/10.2134/jeq2013.11.0466.

Geeska Afrika Online (2020). Ethiopia: Koysha hydropower Dam at 39% complete. https://www.geeskaafrika.com/koysha-hydropower-dam-39/ (Accessed:2021-07-04).

Georgiou, P., & Papamichail, D. (2008). Optimization model of an irrigation reservoir for water allocation and crop planning under various weather conditions. *Irrigation science*, *26*(6), 487–504.

Giuliani, M., Anghileri, D., Castelletti, A., Vu, P. N., & Soncini-Sessa, R. (2016a). Large storage operations under climate change: expanding uncertainties and evolving trade-offs. *Environmental Research Letters*, *11*(3), 035009.

Giuliani, M., Castelletti, A., Pianosi, F., Mason, E., & Reed, P. M. (2016b). Curses, trade-offs, and scalable management: Advancing evolutionary multiobjective direct policy search to improve water reservoir operations. *Journal of Water Resources Planning and Management*, *142*(2), 04015050.

Goodland, R. (2010). The World Bank Versus the World Commission on Dams. *3*(2), 15.

Gownaris, N. J., Pikitch, E. K., Ojwang, W. O., Michener, R., & Kaufman, L. (2015). Predicting species vulnerability in a massively perturbed system: The fishes of lake turkana, kenya. *PloS one*, *10*(5), e0127027.

Graf, W. L. (2001). *Dam* age Control: Restoring the Physical Integrity of Americas Rivers. *Annals of the Association of American Geographers*, *91*(1), 1–27.

Gupta, H. V., Kling, H., Yilmaz, K. K., & Martinez, G. F. (2009). Decomposition of the mean squared error and nse performance criteria: Implications for improving hydrological modelling. *Journal of hydrology*, *377*(1-2), 80–91.

Gyasi, S. F., Boamah, B., Awuah, E., & Otabil, K. B. (2018). A Perspective Analysis of Dams and Water Quality: The Bui Power Project on the Black Volta, Ghana. *Journal of Environmental and Public Health*, *2018*, 6471525.

Hadka, D., & Reed, P. (2013). Borg: An auto-adaptive many-objective evolutionary computing framework. *Evolutionary computation*, *21*(2), 231–259.

Hadka, D., & Reed, P. (2015). Large-scale parallelization of the borg multiobjective evolutionary algorithm to enhance the management of complex environmental systems. *Environmental Modelling & Software*, *69*, 353–369.

Hall, J. W., Grey, D., Garrick, D., Fung, F., Brown, C., Dadson, S. J., & Sadoff, C. W. (2014). Coping with the curse of freshwater variability. *Science*, *346*(6208), 429–430.

HarvestChoice (2014). Crop production: Spam.

Hathaway, T. (2009). Facing gibe 3 dam: Indigenous communities of ethiopias lower omo valley. *International Rivers*.

Ho, M., Lall, U., Allaire, M., Devineni, N., Kwon, H. H., Pal, I., Raff, D., & Wegner, D. (2017). The future role of dams in the United States of America. *Water Resources Research*, *53*(2), 982–998. _eprint: https://agupubs.onlinelibrary.wiley.com/doi/pdf/10.1002/2016WR019905.

Hodbod, J., Stevenson, E. G., Akall, G., Akuja, T., Angelei, I., Bedasso, E. A., Buffavand, L., Derbyshire, S., Eulenberger, I., Gownaris, N., et al. (2019). Social-ecological change in the omo-turkana basin: A synthesis of current developments. *Ambio*, *48*(10), 1099–1115.

Hu, M., & Huang, Y. (2020). atakrig: An R package for multivariate area-to-area and area-to-point kriging predictions. *Computers & Geosciences*, *139*, 104471.

Human Rights Watch (2017). Ethiopia: Dams, plantations a threat to kenyans.

Huntington, T. G. (2006). Evidence for intensification of the global water cycle: Review and synthesis. *Journal of Hydrology*, *319*(1-4), 83–95.

Hurford, A. P., & Harou, J. J. (2014). Balancing ecosystem services with energy and food security Assessing trade-offs from reservoir operation and irrigation investments in Kenya's Tana Basin. *Hydrology and Earth System Sciences*, *18*(8), 3259–3277.

IEA (2016). Electricity access database.

IUCN (2018). https : / / www . iucn . org / news / iucn-42whc / 201806 / lake-turkana-listed-danger-due-impacts-dam-advised-iucn.

IUCN Water (2019). The future of dams: Viable options or stranded assets.

Jasperse, J., Ralph, M., Anderson, M., Brekke, L. D., Dillabough, M., Dettinger, M. D., Haynes, A., Hartman, R., Jones, C., Forbis, J., et al. (2017). Preliminary viability assessment of lake mendocino forecast informed reservoir operations. Tech. rep., Center For Western Weather and Water Extremes.

Johnston, L. (2009). Ethiopia - gibe iii hydropower project. trip report.

Kendall, M. G. (1948). Rank correlation methods.

Khan, H. F. (2018). EVALUATING POLICY AND CLIMATE IMPACTS ON WATER RESOURCES SYSTEMS USING COUPLED HUMAN-NATURAL MODELS. (p. 200).

Koutsoyiannis, D., & Economou, A. (2003). Evaluation of the parameterization-simulation-optimization approach for the control of reservoir systems. *Water Resources Research*, *39*(6).

Kroll, C. N., Croteau, K. E., & Vogel, R. M. (2015). Hypothesis tests for hydrologic alteration. *Journal of Hydrology*, *530*, 117–126.

Lee, S., Sadeghi, A. M., Yeo, I.-Y., McCarty, G. W., & Hively, W. D. (2017). Assessing the impacts of future climate conditions on the effectiveness of winter cover crops in reducing nitrate loads into the chesapeake bay watersheds using the swat model. *Transactions of the ASABE*, *60*(6), 1939–1955.

Li, H., Sheffield, J., & Wood, E. F. (2010). Bias correction of monthly precipitation and temperature fields from Intergovernmental Panel on Climate Change AR4 models using equidistant quantile matching. *Journal of Geophysical Research: Atmospheres*, *115*(D10). _eprint: https://agupubs.onlinelibrary.wiley.com/doi/pdf/10.1029/2009JD012882.

Li, Y., Cui, Q., Li, C., Wang, X., Cai, Y., Cui, G., & Yang, Z. (2017). An improved multi-objective optimization model for supporting reservoir operation of China's South-to-North Water Diversion Project. *Science of The Total Environment*, *575*, 970–981.

Liermann, C. R., Nilsson, C., Robertson, J., & Ng, R. Y. (2012). Implications of Dam Obstruction for Global Freshwater Fish Diversity. *BioScience*, *62*(6), 539–548.

Loucks, D. P., & van Beek, E. (2017). *Performance Criteria*, (pp. 375–415). Cham: Springer International Publishing.

Lumbroso, D. M., Woolhouse, G., & Jones, L. (2015). A review of the consideration of climate change in the planning of hydropower schemes in sub-Saharan Africa. *Climatic Change*, *133*(4), 621–633.

Mann, H. B. (1945). Nonparametric tests against trend. *Econometrica: Journal of the econometric society*, (pp. 245–259).

MDI Consulting Engineers (2016). Koysha hydroelectric project, tech. rep., federal democratic republic of ethiopia, ethiopian electric power.

Nachtergaele, F., FAO, IIASA, ISRIC, ISSCA, & JRC (2009). Harmonized world soil database.

NASA JPL (2013). Nasa shuttle radar topography mission global 1 arc second data set.

Neitsch, S. L., Arnold, J. G., Kiniry, J. R., & Williams, J. R. (2011). Soil and water assessment tool theoretical documentation version 2009. Tech. rep., Texas Water Resources Institute.

Oakland Institute (2011). Understanding land investment deals in africa, half a million lives threatened by land development for sugar plantations in lower omo.

Oakland Institute (2019). Massacres in lower omo, ethiopia, call for urgent action by the nobel laureate pm abiy ahmed.

Olden, J. D., Konrad, C. P., Melis, T. S., Kennard, M. J., Freeman, M. C., Mims, M. C., Bray, E. N., Gido, K. B., Hemphill, N. P., Lytle, D. A., McMullen, L. E., Pyron, M., Robinson, C. T., Schmidt, J. C., & Williams, J. G. (2014). Are large-scale flow experiments informing the science and management of freshwater ecosystems? *Frontiers in Ecology and the Environment*, *12*(3), 176–185. _eprint: https://esajournals.onlinelibrary.wiley.com/doi/pdf/10.1890/130076.

Pierce, D. W., Cayan, D. R., Maurer, E. P., Abatzoglou, J. T., & Hegewisch, K. C. (2015). Improved Bias Correction Techniques for Hydrological Simulations of Climate Change. *Journal of Hydrometeorology*, *16*(6), 2421–2442. Publisher: American Meteorological Society Section: Journal of Hydrometeorology.

Pierce, D. W., Cayan, D. R., & Thrasher, B. L. (2014). Statistical downscaling using localized constructed analogs (loca). *Journal of Hydrometeorology*, *15*(6), 2558–2585.

Poff, N. L., Brown, C. M., Grantham, T. E., Matthews, J. H., Palmer, M. A., Spence, C. M., Wilby, R. L., Haasnoot, M., Mendoza, G. F., Dominique, K. C., & Baeza, A. (2016). Sustainable water management under future uncertainty with eco-engineering decision scaling. *Nature Climate Change*, *6*(1), 25–34. Bandiera_abtest: a Cg_type: Nature Research Journals Number: 1 Primary_atype: Reviews Publisher: Nature Publishing Group Subject_term: Climate-change ecology Subject_term_id: climate-change-ecology.

Poff, N. L., & Hart, D. D. (2002). How Dams Vary and Why It Matters for the Emerging Science of Dam Removal: An ecological classification of dams is needed to characterize how the tremendous variation in the size, operational mode, age, and number of dams in a river basin influences the potential for restoring regulated rivers via dam removal. *BioScience*, *52*(8), 659–668.

Quinn, J. D., Reed, P. M., Giuliani, M., Castelletti, A., Oyler, J. W., & Nicholas, R. E. (2018). Exploring How Changing Monsoonal Dynamics and Human Pressures Challenge Multireservoir Management for Flood Protection, Hydropower Production, and

Agricultural Water Supply. *Water Resources Research*, *54*(7), 4638–4662. _eprint: https://agupubs.onlinelibrary.wiley.com/doi/pdf/10.1029/2018WR022743.

Ragettli, S., Cortés, G., McPhee, J., & Pellicciotti, F. (2014). An evaluation of approaches for modelling hydrological processes in high-elevation, glacierized andean watersheds. *Hydrological Processes*, *28*(23), 5674–5695.

Riggs, H. (1980). Characteristics of low flows. *Journal of the Hydraulics Division*, *106*(5), 717–731.

Sabo, J. L., Ruhi, A., Holtgrieve, G. W., Elliott, V., Arias, M. E., Ngor, P. B., Räsänen, T. A., & Nam, S. (2017). Designing river flows to improve food security futures in the Lower Mekong Basin. *Science*, *358*(6368), eaao1053.

Schmitt, R. J., Bizzi, S., Castelletti, A., & Kondolf, G. (2018). Improved trade-offs of hydropower and sand connectivity by strategic dam planning in the mekong. *Nature Sustainability*, *1*(2), 96–104.

Schneller, G., & Sphicas, G. (1983). Decision making under uncertainty: Starr's domain criterion. *Theory and Decision*, *15*(4), 321–336.

SOGREAH (2010). Independent review and studies regarding the environmental & social impact assessments for the gibe iii hydropower project, draft final report.

Starr, M. (1963). Product design and decision theory, prentical hall. *Inc., Englewoods, NJ*.

Steinschneider, S., & Brown, C. (2012). Dynamic reservoir management with real-option risk hedging as a robust adaptation to nonstationary climate. *Water Resources Research*, *48*(5).

Suen, J.-P., & Eheart, J. W. (2006). Reservoir management to balance ecosystem and human needs: Incorporating the paradigm of the ecological flow regime. *Water Resources Research*, *42*(3). _eprint: https://agupubs.onlinelibrary.wiley.com/doi/pdf/10.1029/2005WR004314.

Sundin, C. (2017). Exploring the water-energy nexus in the omo river basin: a first step toward the development of an integrated hydrological-osemosys energy model.

Talbot, C. A., Ralph, M., Jasperse, J., & Forbis, J. (2017). Forecast-informed reservoir operations: Lessons learned from a multi-agency collaborative research and operations effort to improve flood risk management, water supply and environmental benefits. In *AGU Fall Meeting Abstracts*, vol. 2017, (pp. H11J–1338).

Tiwari, H., Rai, S. P., Sharma, N., & Kumar, D. (2017). Computational approaches for annual maximum river flow series. *Ain Shams Engineering Journal*, *8*(1), 51–58.

Tolson, B. A., & Shoemaker, C. A. (2006). The Dynamically Dimensioned Search (DDS) Algorithm as a Robust Optimization Tool in Hydrologic Modeling. *AGU Fall Meeting Abstracts*, *2006*, H41I–07.

Trenberth, K. E. (2011). Changes in precipitation with climate change. *Climate Research*, *47*(1-2), 123–138.

USACE (2007). *HEC-ResSim Reservoir System Simulation User's Manual*. U.S. Army Corps of Engineers.

Wang, R., Bowling, L. C., & Cherkauer, K. A. (2016). Estimation of the effects of climate variability on crop yield in the midwest usa. *Agricultural and Forest meteorology*, *216*, 141–156.

Watts, R. J., Richter, B. D., Opperman, J. J., & Bowmer, K. H. (2011). Dam reoperation in an era of climate change. *Marine and Freshwater Research*, *62*(3), 321–327. Publisher: CSIRO PUBLISHING.

Wild, T. B., Reed, P. M., Loucks, D. P., Mallen-Cooper, M., & Jensen, E. D. (2019). Balancing Hydropower Development and Ecological Impacts in the Mekong: Tradeoffs for Sambor Mega Dam. *Journal of Water Resources Planning and Management*, *145*(2), 05018019. Publisher: American Society of Civil Engineers.

Woodroofe, R. (1996). Omo-gibe river basin integrated development master plan study final report vol. iii. *VI Water resources Surveys and Inventories, ministry of Water Resources, Addis Ababa*.

Wu, J., Yen, H., Arnold, J. G., Yang, Y. C. E., Cai, X., White, M. J., Santhi, C., Miao, C., & Srinivasan, R. (2020). Development of reservoir operation functions in SWAT+ for national environmental assessments. *Journal of Hydrology*, *583*, 124556.

Yu, Y., Zhao, R., Zhang, J., Yang, D., & Zhou, T. (2021). A multi-objective game optimization for balancing economic, social and ecological benefits in the Three Gorges Reservoir operation. *Environmental Research Letters*.

Zagona, E. A., Fulp, T. J., Shane, R., Magee, T., & Goranflo, H. M. (2001). Riverware: A generalized tool for complex reservoir system modeling 1. *JAWRA Journal of the American Water Resources Association*, *37*(4), 913–929.

Zaniolo, M., Giuliani, M., Sinclair, S., Burlando, P., & Castelletti, A. (2021). When timing mattersmisdesigned dam filling impacts hydropower sustainability. *Nature Communications*, *12*(1), 3056. Number: 1 Publisher: Nature Publishing Group.

Zarfl, C., Lumsdon, A. E., Berlekamp, J., Tydecks, L., & Tockner, K. (2015). A global boom in hydropower dam construction. *Aquatic Sciences*, *77*(1), 161–170.

Zeff, H. B., Herman, J. D., Reed, P. M., & Characklis, G. W. (2016). Cooperative drought adaptation: Integrating infrastructure development, conservation, and water transfers into adaptive policy pathways. *Water Resources Research*, *52*(9), 7327–7346. _eprint: https://agupubs.onlinelibrary.wiley.com/doi/pdf/10.1002/2016WR018771.

Zhang, X., Li, H.-Y., Deng, Z. D., Ringler, C., Gao, Y., Hejazi, M. I., & Leung, L. R. (2018). Impacts of climate change, policy and water-energy-food nexus on hydropower development. *Renewable Energy*, *116*, 827–834.